Title

Understanding the causes and consequences of past marine carbon cycling variability through models

Journal

Earth-Science Reviews, 171(Geochem. Geophys. Geosyst.62005)

ISSN

0012-8252

Authors

Hülse, Dominik
Arndt, Sandra
Wilson, Jamie D
et al.

Publication Date

2017-08-01

DOI

10.1016/j.earscirev.2017.06.004

Peer reviewed

Manuscript prepared for *Earth-Science Reviews*

Date: 3 March 2017

Understanding the ocean's biological carbon pump in the past: Do we have the right tools?

Dominik Hülse[1], Sandra Arndt[1], Jamie D. Wilson[1], Guy Munhoven[2], and Andy Ridgwell[1, 3]

[1]School of Geographical Sciences, University of Bristol, Clifton, Bristol BS8 1SS, UK

[2]Institute of Astrophysics and Geophysics, University of Liège, B-4000 Liège, Belgium

[3]Department of Earth Sciences, University of California, Riverside, CA 92521, USA

Correspondence to: D. Hülse (Dominik.Huelse@bristol.ac.uk)

Keywords: Biological carbon pump; Earth system models; Ocean biogeochemistry; Marine sediments; Paleoceanography

Abstract. The ocean is the biggest carbon reservoir in the surficial carbon cycle and, thus, plays a crucial role in regulating atmospheric CO_2 concentrations. Arguably, the most important single component of the oceanic carbon cycle is the biologically driven sequestration of carbon in both organic and inorganic form- the so-called biological carbon pump. Over the geological past, the intensity of the biological carbon pump has experienced important variability linked to extreme climate events and perturbations of the global carbon cycle. Over the past decades, significant progress has been made in understanding the complex process interplay that controls the intensity of the biological carbon pump. In addition, a number of different paleoclimate modelling tools have been developed and applied to quantitatively explore the biological carbon pump during past climate perturbations and its possible feedbacks on the evolution of the global climate over geological timescales. Here we provide the first, comprehensive overview of the description of the biological carbon pump in these paleoclimate models with the aim of critically evaluating their ability to represent past marine carbon cycle dynamics. First, the paper provides an overview of paleoclimate models and paleo-applications for a selection of Earth system box models and Earth system Models of Intermediate Complexity (EMICs). Secondly, the paper reviews and evaluates three key processes of the marine organic and inorganic carbon cycling and their representation in the discussed paleoclimate models: biological productivity at the ocean surface, remineralisation/dissolution of particulate carbon within the water column and the benthic-pelagic coupling at the seafloor. Illustrative examples using the model GENIE show how different parameterisations of water- column and sediment processes

can lead to significantly different model results. The presented compilation reveals that existing paleoclimate models tend to employ static parametrisations of the biological carbon pump that are empirically derived from present-day observations. These approaches tend to represent carbon transfer in the modern ocean well; however, their empirical nature compromises their applicability to past climate events characterized by fundamentally different environmental conditions. GENIE results show that paleoclimate models may for instance over- or underestimate carbon sequestration in the ocean-sediment system with important implications for the accuracy of the predicted climate response. Finally, the paper discusses the importance of using models of different complexities and gives suggestions how they can be applied to quantify various model uncertainties.

Contents

1 Introduction

The evolution of global climate on geological timescales can be viewed as a series of warm and cold periods that are associated with variations in atmospheric carbon dioxide (CO_2) concentrations. Over long timescales ($> 10^6$ years) the climate system is driven by a dynamic balance between varying CO_2 inputs from volcanoes and metamorphic alteration of rock, and the removal of CO_2 from the ocean-atmosphere system through weathering and burial of carbon in marine sediments (e.g. **????**). An important aspect of paleoclimate studies and in particular numerical modelling, is to quantify the dynamic balance between carbon sources and sinks and its possible feedbacks on the evolution of the global climate over various timescales. The oceans and the surface sediments contain the largest carbon reservoir within the surficial Earth system ($\sim$38,850 Pg C) and are therefore essential for understanding the global carbon cycle and climate on timescales longer than > 100 years (**????**). On even longer timescales (more than 100,000 years) deeply buried sediments and crustal rocks provide the ultimate long-term sink for CO_2 which is balanced by volcanic degassing (**?**, Fig. 1). The formation of biogenic particles and their fate within the water column and sediments, the biological pump, is a key link between different carbon reservoirs with processes operating on a range of timescales from plankton growth/death on the order of hours to days to the dissolution of $CaCO_3$ in the sediments over 100,000 years.

In the modern carbon cycle the net removal of CO_2 from the atmosphere to the oceans and sediments is almost entirely a direct consequence of the combined effect of the solubility and biological pump (**?**). The solubility pump (which is not further investigated in this paper) describes the air-sea gas exchange of CO_2 and is estimated to account for only $\sim$10% of the surface-to-deep gradient of (preindustrial) dissolved inorganic carbon (DIC) (**?**). The biological carbon pump refers in this paper to both, the organic and inorganic carbon fixed by primary producers in the euphotic zone and exported to the ocean below, where it is respired, dissolved or buried in the sediments (Fig. 2; **?**). The growth of phytoplankton in the light-flooded surface layer of the global ocean removes nutrients and carbon from the water and transforms them into cellular material and/or inorganic carbonates. Upon organism death, part of this produced particulate organic and inorganic carbon (POC, PIC) sinks out of the euphotic zone. In addition, dissolved organic carbon (DOC) is either scavenged by particle aggregates and sinks to the deep ocean or is redistributed into the deeper layers by ocean circulation. In today's well oxidised ocean a large fraction of the gross primary production of organic matter is remineralised by bacterial activity in the water column and less than $\sim 0.5\%$ of it is ultimately

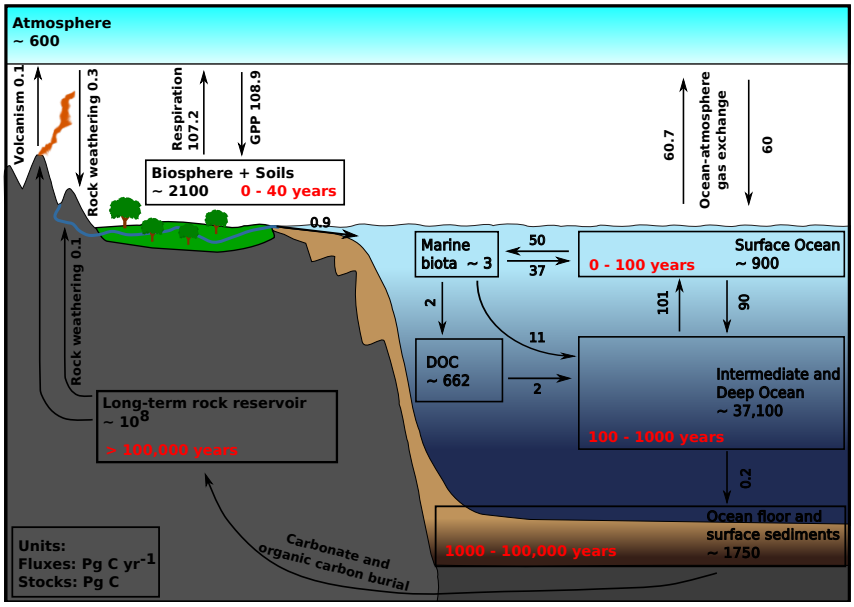

Figure 1: A simplified view of the global carbon cycle showing the approximate carbon stocks in Pg C and main annual fluxes in Pg C yr^{-1} for the preindustrial era (largely based on IPCC 2013 (**?**) and **?**, GPP: Gross Primary Production). Years in red indicate the timescales at which the reservoirs exert control on atmospheric CO_2 concentrations. Thus, the biological carbon pump in the ocean is important on timescales shorter than about 1000 years, whereas the sediments become influential on timescales of 1000 to 100,000 years.

buried in marine sediments (Fig. 1; **??**). Despite intense ocean upwelling and mixing, the biological pump results in distinct ocean depth gradients of carbon, nutrients and oxygen. In particular its control on surface ocean DIC concentration, which is next to temperature, wind speed and ambient pH one of the main drivers of air-sea carbon dioxide fluxes, is of fundamental importance for the global carbon cycle and thus global climate (**?**). In fact, modelling studies have shown that atmospheric CO_2 concentrations would be significantly higher above an abiotic ocean (**??**). **?** show that the organic part of the biological pump is responsible for about 70% and the inorganic part for 20% of the total preindustrial dissolved inorganic carbon transfer from the surface to the deeper ocean. The remaining 10% are attributed to DIC variations driven by temperature variations, ocean mixing and the solubility pump.

The efficiency of the biological pump depends not only on the rate of carbon fixation and export out of the surface layer, but also on the depth at which the organic and inorganic carbon is respired

or dissolved. This depth determines the time during which carbon is isolated from the atmosphere and therefore atmospheric CO_2 concentration exhibits an inverse relationship to the efficiency of the biological pump (**??**). Estimates for global organic carbon exported from the surface to the deeper ocean are in the range of 5-11 Pg C yr^{-1} (**???**). In the contemporary, well-oxygenated ocean, only a small fraction of the carbon organically produced in the surface ocean escapes microbial degradation (remineralisation) and is eventually buried in the sediment (e.g. **?**). This imbalance between photosynthesis and degradation has been of major importance to life on Earth because it enabled accumulation of molecular oxygen in the atmosphere and the storage of organic matter in sediments over a period of at least the last two billion years (e.g. **??**). The inorganic carbon flux is strongly coupled to the organic carbon flux by the biologically driven carbonate precipitation and the effect of organic matter remineralisation on carbonate preservation (see Box 1 or, e.g., **??**). The complex interplay and the strong feedbacks between fluxes and transformations of carbon in the ocean-sediment system limit our predictive ability of the global climate system and its evolution throughout Earth's history (**?**).

In general, it is extremely difficult to disentangle the underlying physical and biogeochemical process interplay from observations that simply reflect the net process outcome. Appropriate mathematical models can help as they provide the ability to trace various rates of biogeochemical processes and related fluxes. They also present the opportunity to quantitatively test hypotheses that arise from observations. Therefore, mathematical models are very useful tools to explore and quantify the carbon cycling through the ocean-sediment system, as well as implications for the global climate evolution. The model-supported analysis of global carbon cycling started in the mid-fifties with the box-models of **?**, **?** and **?**. **?** further added a diffusive representation of carbon transport in the sea, thus producing the first so-called box-diffusion models. **?** adopted the box-modelling framework to the steady-state long-term rock cycle. Time-dependent quantitative simulation experiments about the role of the carbonate and silicate rock cycles for the evolution of atmospheric CO_2 were realized with the BLAG model (**?**). This was the first in a long line of box-models often referred to as *Berner models* (**???**).

Box-diffusion models and variants thereof became widely used in the seventies and early eighties to study the partitioning of anthropogenic CO_2 between the atmosphere and the sea (**????**). Early investigations on the glacial-interglacial CO_2 variations documented in the ice-cores relied again on simple three- to four-box models (**??????**, to cite only a few pre-1985 papers). These models were

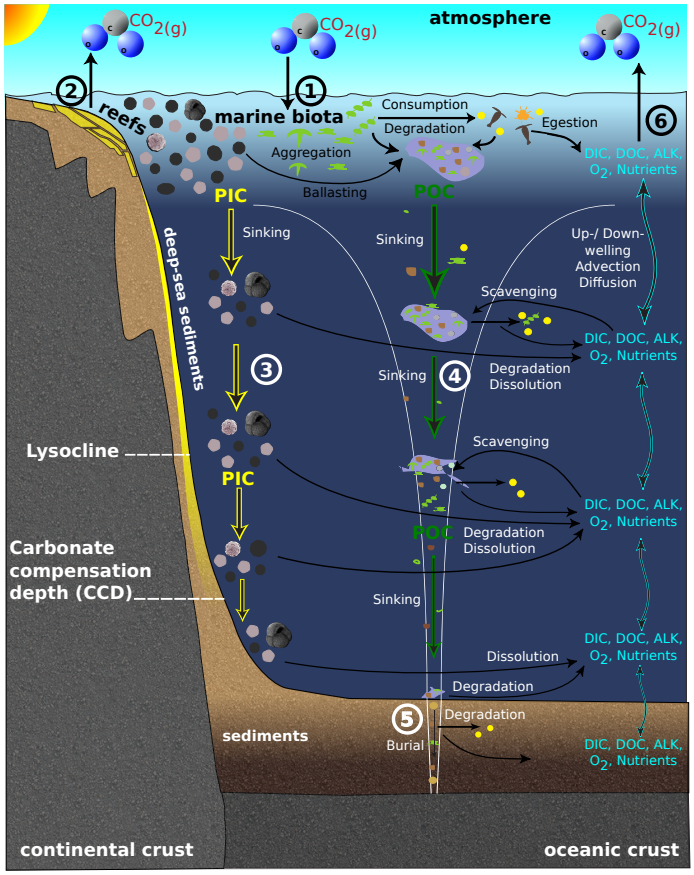

Figure 2: Schematic of the main processes constituting the ocean's solubility and biological pumps (labelled 1 to 6). **1**: Air-sea gas exchange of CO_2, used by phytoplankton to form cellular material. Through complex recycling and aggregation pathways, agglomerations of POC and PIC are formed, heavy enough to sink out of the euphotic zone. **2**: Precipitation of $\mathrm{CaCO_3}$ by, e.g., coccolithophores and foraminifera in the open ocean or by corals and coralline algae in the shallow-water contributing to the formation of reefal structures, resulting in higher $\mathrm{pCO_2}$ at the surface and therefore a transfer of CO_2 to the atmosphere. ($\mathrm{Ca^{2+} + 2HCO_3^- \rightarrow CaCO_3 + CO_{2(aq)} + H_2O}$). **3**: Carbonate sinking into the deeper ocean and forming deep-sea sediments. At the lysocline the rate of dissolution increases dramatically until below the CCD no $\mathrm{CaCO_3}$ is present in the sediment any more. **4**: Vertical settling flux of POC (in combination with PIC) that decreases approximately exponentially with depth. **5**: Deposition of organic carbon in the deep sea. Only a small fraction escapes degradation and is buried in the sediments. **6**: DIC in the upper ocean is created through degradation and egestion processes and upwelling of DIC rich subsurface waters. These processes contribute to raise surface water $\mathrm{pCO_2}$, driving a transfer of CO_2 to the atmosphere.

also the first ones to explicitly consider the surface to deep-sea transport of carbon by biogenic particles. The term "biological pump" was also coined at about that time (**?**). Later, configurations with a larger number of boxes came into usage: the 13-box CYCLOPS (**?**); the ten-box PANDORA (**?**); the ten-box model of **??**, and the 19-box model of **?** (only oceanic reservoirs considered). Including a larger number of boxes helped on one hand to resolve the major ocean basins and water masses, but, on the other hand, increased the number of free parameters in the models (mainly the water exchange fluxes between the reservoirs) and thus made them more and more difficult to calibrate. In the mean time, the first three-dimensional ocean carbon cycle model had made its appearance (**??**). The physically-based water circulation field that these models were based upon could be used to overcome the calibration dilemma of the multi-box models mentioned above (**???**). Box-models fell somewhat in disgrace after **?** had shown that they had a considerably higher sensitivity to high-latitude changes than two- or three-dimensional models, questioning the applicability of box-models for the quantitative assessment of the effects of high-latitude changes of biogeochemical and physical processes on atmospheric pCO_2. **?** finally demonstrated that the high-latitude sensitivity diagnosed by **?** is not related to the model type (box, versus 2D or 3D), but rather to the way the models are constructed. During the nineties, faster processors and improved data storage devices progressively allowed the application of increasingly resolved models with increasingly improved physics on geological relevant time scales. In particular, coupled, multi-dimensional paleoclimate models, so-called Earth System Models of Intermediate Complexity (EMIC) have emerged in response to the rapid increase in computer power. As a result, box-models have to some extent been superseded by EMICs, especially, for the study of scientific problems that involve changing water mass distributions, which are difficult to take into account in a consistent and mechanistic way in box-models, or if vertical re-distributions of fluxes or solute materials must be tracked. Box-models nevertheless remain indispensable tools to analyse and interpret the results of more complex 2D and 3D models (**?**) and to improve our general process understanding (e.g. **?**). They also continue to be used as research tools on their own for time scales of hundreds of millions of years (e.g., **?**), hundreds of thousands of years (e.g., **??**) and future evolution of global carbon cycle (e.g., **??**). Finally, they also continue to be developed (e.g., **?**). The **?** model was even revised and extended after more than thirty years to yield a new model, called MAGic (**?**). MAGic is unique in that it uses thermodynamic constants for its pH calculations that are based upon Pitzer equations, which are not biased towards the present-day sea salt composition, but can cope on varying composition.

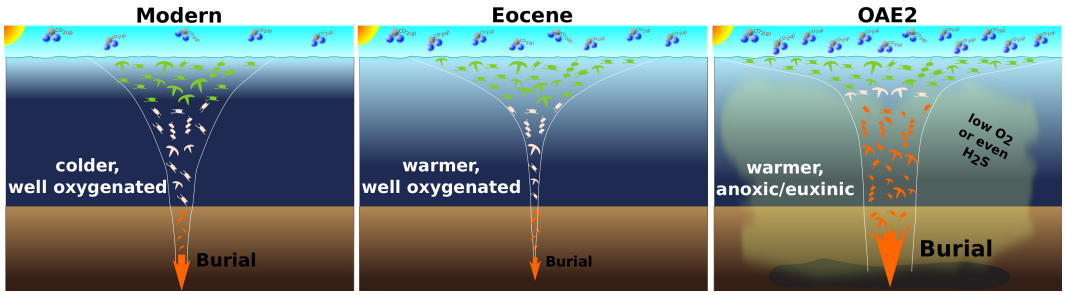

Figure 3: Schematic representation of the potential functioning of the biological pump in the modern world (left), during the Eocene (middle) and the oceanic anoxic event 2 (right, OAE2). There is much evidence that global mean ocean temperatures exceeded those of the modern day by several degrees during the Eocene epoch (55.5-33.7 Ma) and theory predicts that elevated temperatures should cause a decrease in the efficiency of the biological pump as sinking POC is more quickly remineralised. In contrast, during OAE2 (ca. 93.5 Ma) the ocean exhibited widespread oxygen depletion and photic zone euxinia (occurrence of hydrogen sulfide (H_2S)). At the same time the marine sediments are characterised by enhanced deposition of organic carbon-rich black layers.

The cycling of both organic and inorganic carbon through the ocean-sediment system is driven by a complex interplay of biogeochemical processes. As opposed to much of the ocean physical dynamics, there is no fundamental theoretical framework for the description of these complex marine biogeochemical dynamics. Because of temporal and spatial constraints, unconstrained boundary conditions, excessive computational costs, but also simply because of the lack of mechanistic knowledge, paleoclimate models cannot capture the full complexity of the real carbon cycle (**???**). Therefore, processes are often parametrised or neglected. Although such simplification is necessary it should ideally be based on a mechanistic understanding of the underlying processes. The applicability of parametrisations that are derived from observations of the present-day ocean-sediment system is particularly critical in the case of paleoclimate models, since observations are obtained under environmental conditions that are largely different from the ones that most likely prevailed during past extreme events (compare Fig. 3).

Unlike in the case of ocean-atmosphere dynamics, there has not yet been any review study of the marine carbon cycle dynamics in paleoclimate models, a process which could help to substantially upgrade the performance of these models and raise the degree of confidence in their results. Although commonly not considered as part of the biological carbon pump, sediment dynamics are

discussed as part of the benthic-pelagic coupling in this review as they play an important role for carbon cycling and Earth's recovery from global warming events, especially on longer timescales (> 100 years; Fig. 1). Conversely, the impact of ocean circulation on the biological carbon pump is not included as it is not a direct factor influencing its dynamics. Furthermore, this study does not aim to provide an exhuastive review of all critical aspects of ocean biogeochemistry, which would be hardly feasible. It rather focusses on three key aspects of marine organic and inorganic carbon cycling and their encapsulation into Earth system models: biological productivity at the ocean surface, remineralisation/dissolution of carbon within the water column and the benthic-pelagic coupling at the seafloor. The core problem addressed here is the range of formulations used to represent these key carbon cycle processes and the resulting divergence of predictions for carbon cycle change under different boundary conditions, such as increased global temperatures, ocean anoxia or euxinia (Fig. 3).

First, different types of paleoclimate models are presented and compared; and an overview for their characteristic timescales of application is given (Section 2). The criteria applied for selecting the models are summarised in Table 1. Thereafter, the focus of the paper is on reviewing the three key processes of the biological carbon pump and evaluating their representation in paleoclimate models by testing their ability to predict the response of carbon cycling under different extreme climate conditions (Section 3). The final part (Section 4), highlights the importance for applying models of different complexities, gives suggestions how these models can be applied to explore and quantify different model uncertainties, and summarises two key outstanding modelling issues.

Table 1: Criteria for selection of Box models and EMICs for this study (all must be satisfied).

Criteria	**Description**
Biological pump	Models including an ocean circulation model with a minimum set of components to facilitate the representation of the biological pump (e.g. biological uptake of tracers, export production, remineralisation in the water column).
Ocean resolution	Three-dimensional with a resolution lower than $2^\circ \times 2^\circ$ or at least represented by 10 homogeneous boxes or three zonally averaged ocean basins.
Applications	The model must have been applied to at least two different paleo-events or used in two different studies on the same event with a focus on biogeochemical processes in the ocean.

2 Paleoclimate Earth system models

Numerical models are important tools that help us to understand the complex Earth system dynamics, including how climate and the biological pump have changed in the past and how they may evolve in the future (see e.g. **???**). Existing Earth system models vary considerably in complexity from highly parametrised conceptual models (e.g., box models) to comprehensive coupled General Circulation Models (GCMs) and different scientific questions are tackled with different model approaches. GCMs encompass sophisticated representations of global atmosphere and ocean circulation and describe many details of fluxes between the ocean-atmosphere systems (see e.g. **?**). Newer GCMs also include refined ocean biogeochemistry models (e.g. PISCES (**?**) and HAMOCC (**?**)) but are mainly used to study biogeochemistry in the modern ocean. Historically, paleoclimate models with a focus on the ocean's biological pump have evolved along two distinct paths. Earth system box models were designed around simplified multi-box or advection-diffusion models of the ocean circulation, while Earth System Models of Intermediate Complexity (EMICs; **?**) can be considered as coarse resolution Earth system models (e.g. **?**). Writing a comprehensive review of all available models representing the biological pump would be an impossible task. Here we have chosen to focus on more computationally efficient models, such as box models (Section 2.1) and intermediate complexity models (Section 2.2) with a minimum set of components to facilitate the representation of the biological carbon pump. All selected models have been used to study biogeochemical cycling in Earth history and allow to run simulations for tens of thousands of years, thus are able to model processes involving the deep ocean and the marine sediments (compare Table 1). GCMs, employing a complex ocean biogeochemistry model, are not included in this review as their application is generally limited to the modern ocean and/or to short timescales due to their high resolution and complexity (yet, see e.g. **?**, for a paleo-study using HAMOCC in a fully coupled GCM).

2.1 Earth system box models

Earth system box models are a very conceptualised representations of the Earth system and are employed to test hypotheses and to quantify large scale processes. Due to their high computational efficiency they allow the investigation of long-term dynamics in the Earth system and its biogeochemical evolution (compare Fig. 4). **?** for instance, simulated with a simple 4-box model of the ocean-atmosphere the substantial influence of high latitude surface ocean productivity and thermohaline overturning rate on atmospheric CO_2 fluctuations during glacial-interglacial cycles. However,

Earth system box models incorporate highly simplified representations of both the atmosphere and ocean systems with the notable exception of the GEOCLIM family of models which use the biogeochemical ocean-atmosphere model COMBINE (**?**) and couple it to the three-dimensional climate model FOAM (**?**). In general, the atmosphere is encapsulated into a simple one-box model and atmospheric processes are reduced to simple gas and sometimes heat exchange (e.g., DCESS **?**). Without a fully-resolved atmosphere, the upper oceanic boundary conditions (wind stress, heat flux, equilibrium state with fixed boundary conditions and fresh-water flux) can also not be defined in a physically rigorous way. Therefore, the representation of ocean circulation in these models is highly parametrised and ranges from simple multi-box models with prescribed exchange fluxes (e.g., BICYCLE, **?**) to advection-diffusion box models (e.g., GEOCLIM *reloaded*, **?**). Ice sheet dynamics are generally neglected due to the simplicity of the ocean-atmosphere models. Terrestrial vegetation and weathering fluxes are generally integrated in form of simplified rate laws (e.g., BICYCLE; **?**).

2.2 Earth system Models of Intermediate Complexity

Another class of so-called Earth system Models of Intermediate Complexity (**?**) have been developed to close the gap between the computationally efficient, but conceptual box models and the computationally expensive general circulation models. The first EMIC-like models that already included and coupled important parts of the Earth system were developed in the early 1980s (**??**). The spatial resolution of EMICs is coarser than that of "state-of-the-art" GCMs. However, they explicitly simulate, in an interactive mode, the basic components of the Earth system, including the atmosphere, ocean, cryosphere and land masses, over a very wide range of temporal scales, from a season to hundreds of thousands and even millions of years. In addition, EMICs include, although often in parametrised form, most of the processes described in GCMs (**?**). On the other hand, they are efficient enough to resolve climate dynamics on the event-scale (kyrs) and are thus especially useful for the study of paleoclimate dynamics since they allow exploring the complex behaviour of Earth's climate system as an integrated multi-component system with non-linearly coupled processes. Often EMICs incorporate more sub-component models (e.g. sediments) and climatic variables than GCMs (**?**). Furthermore, they facilitate large ensemble experiments needed for climate sensitivity studies to external forcings (e.g. **??**) and can provide guidance for more detailed investigations using more complex GCMs. Also, due to their fast computation, EMICs are able to integrate long-term processes like carbonate preservation in marine sediments (**??**) which is important for regulating atmospheric

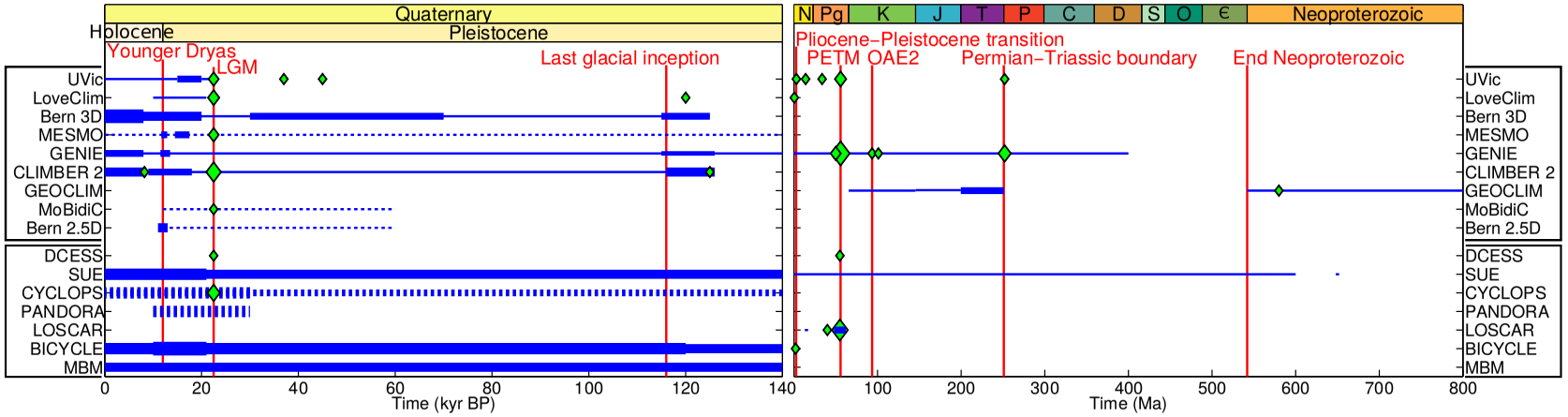

Figure 4: Timeline for EMIC and Earth system box model applications (ordered from higher to lower ocean resolution). Diamonds represent steady-state studies, solid lines display transient simulations for the specific time period and dotted lines steady-state studies for the respective period without a specified time. The size of the diamonds and thickness of the lines reflect the number of studies for this time period (also compare Table 6). The geological timescale abbreviations for the periods are: N: Neogene, Pg: Paleogene, K: Cretaceous, J: Jurassic, T: Triassic, P: Permian, C: Carboniferous, D: Devonian, S: Silurian, O: Ordovician, ∈: Cambrian. Note the change of timescale!

CO_2 concentrations on timescales of thousands to tens of thousands of years (**?**). The model design is generally driven by the underlying scientific questions, the considered temporal and spatial scales, as well as by the expertise of the research group. As a consequence, different components of the climate system are described with different levels of complexity. Most EMICs emerged from comprehensive, dynamic climate models that were used to study contemporary climate change and thus rely on sophisticated coupled ocean-atmosphere GCMs with integrated ice sheet dynamics (e.g. **?**). Terrestrial vegetation and weathering dynamics in EMICs are often included on the basis of dynamic models (such as VECODE in CLIMBER-2; **?**, **?**; or RoKGeM in GENIE; **?**, **?**, respectively). A major caveat of many existing models is the lack of a sophisticated sedimentary biogeochemical model for organic carbon (compare Section 3.3). Notable exceptions are Bern 3D which includes a vertically-integrated, dynamic model considering oxic degradation and denitrification of organic carbon (**?**); the box model MBM, integrating a vertically-resolved advection-diffusion-reaction model for solid and solute species (MEDUSA, **?**); and DCESS, using a semi-analytical, iterative approach considering (oxic and anoxic) organic matter remineralisation (**?**).

3 The Biological Carbon Pump in Models

Over the geological past, the intensity of the biological pump has probably experienced significant spatial and temporal variability that can be directly linked to perturbations of the global carbon cycle and climate (e.g. **????**). Therefore, the description of the biological carbon pump exerts an important control on the performance and predictive abilities of Earth system models. Simulating the ocean's carbon pump is made difficult by the plethora of processes that govern the formation of particulate organic and inorganic carbon (POC, PIC) and dissolved organic carbon (DOC) in the euphotic zone, its export to depth and its subsequent degradation, dissolution or burial in the sediments. Unlike for ocean circulation, a fundamental set of first principle equations that govern nutrient cycling still remains to be defined, assuming they even exist. Thus a wide range of model approaches of varying sophistication have been put forward for specific problems (e.g. **?????**). The following sections critically review important processes of the biological pump and their representation in paleoclimate models. They are separated into biological production in the surface ocean (3.1), carbon dynamics in the deeper ocean (3.2) and benthic processes (3.3). The numerical representations are generally described moving from simple/empirical to more dynamic/mechanistic approaches. Even though the silica cycle is strongly interrelated with the biological pump (e.g. opal as a ballasting material; **?**)

Table 2: Overview of EMICs mentioned in this study and their characteristics related to the biological pump.

Models	Ocean Model Resolution	Ocean Carbon Cycle Surface Production	Ocean Carbon Cycle Tracers	Ocean Carbon Cycle Degradation	Sediments
EMIC					
UVic	3-D, 1.86° (meridional) x 3.6° (zonal), 19 vertical layers	Fully coupled carbon cycle + NPZD ecosystem representation + dynamic iron cycle; e.g. Schmittner et al. (2008), Keller et al. (2012), Nickelsen et al. (2015)	Phytoplankton (nitrogen fixers and others), NO_3, PO_4, O_2, DIC, $CaCO_3$, ALK, zooplankton, particulate detritus, POC, DOC, $\delta^{13}C$, $\delta^{18}O$, Fe, Fe_P	Single exponential	$CaCO_3$ model with oxic-only sediment respiration (Archer, 1996a)
LOVECLIM	3-D, 3° x 3°, 30 vertical layers; Goosse et al. (2010)	Fully coupled carbon cycle; LOCH:Mouchet and Francois (1996); rain ratio depends on silica, tmp, $CaCO_3$)	DIC, Alkalinity, dissolved inorganic phosphorous, DOC, POC, O_2, org. and inorg. $\delta^{13}C$, $\delta^{18}O$, $CaCO_3$, silica, opal	Power law (Martin)	Constant part of POC & PIC is preserved; Goosse et al. (2010)
Bern 3D	3-D, horizontal 36x36 equal area boxes, 10°x(3.2-19.2)°, 32 vertical layers; Müller et al. (2006)	Fully coupled carbon cycle, Michaelis-Menten nutrient uptake kinetics, limited by PO_4, Fe and light. Parekh et al. (2008); Tschumi et al. (2008)	CFC-11, PO_4, DOP, DIC, DOC, $\delta^{13}C$, $\delta^{14}C$, $\delta^{39}Ar$, Ar, ALK, O_2, FeT; Müller et al. (2008), Parekh et al. (2008)	Power law (Martin)	Vertically integrated, dynamic model of top 10cm: oxic respiration and denitrification. $CaCO_3$, opal, POM, clay and DIC, ALK, PO_4, NO_3, O_2, silicic acid; Tschumi et al. (2011)
MESMO	3-D, horizontal 36x36 equal area boxes, 10° x (3.2-19.2)°, 16 vertical layers	Fully coupled carbon cycle, Michaelis-Menten nutrient uptake kinetics, limited by PO_4, NO_3, CO_2 , Fe, light and tmp; Matsumoto et al. (2008)	CFC-11, NO_3, N*, ^{15}N, PO_4, O_2, DIC, $CaCO_3$, ALK, POC, DOC, $\delta^{13}C$, ^{14}C	Temp dependent	Vertically integrated model: u.a. $CaCO_3$, detrital material, $\delta^{13}C$, $\delta^{14}C$; Ridgwell and Hargreaves (2007)
GENIE	3-D, horizontal 36x36 equal area boxes, 10° x (3.2-19.2)°, 8/16 vertical layers	Fully coupled carbon cycle, Michaelis-Menten nutrient uptake kinetics, limited by PO_4, NO_3, Fe and light, Ridgwell et al. (2007)	Ca. 56 dissolved and various solid tracers; see www.seao2.info/mycgenie.html	Double Exponential / Temp dependent / Power Law / Ballasting	Vertically integrated model: u.a. $CaCO_3$, detrital material, $\delta^{13}C$, $\delta^{14}C$; Ridgwell and Hargreaves (2007)
CLIMBER-2	3 zonally averaged basins, 2.5° (meridional), 20 vertical layers	Fully coupled carbon cycle (HAMOCC3) + ecosystem model, Six and Maier-Reimer (1996)	DIC, DOC, PO_4, O_2, Alkalinity, silicate, isotopes (^{12}C, ^{13}C, ^{14}C, ^{39}A), $\delta^{18}O$; Brovkin et al. (2002)	Power law (Suess)	$CaCO_3$ model with oxic-only sediment respiration (Archer, 1996a)
GEOCLIM	3 zonally averaged basins, 2.5° (meridional), 20 vertical layers (uses CLIMBER-2)	Fully coupled carbon cycle model, PO_4 limiting nutrient (using COMBINE, Goddéris and Joachimski (2004))	PIC, POC, PO_4, O_2, DIC, ALK, pH, $\delta^{13}C$, $\delta^{18}O$, Ca^{2+}, $CaCO_3$	Recycling rate linear fct of O_2	Simple org. C, P model (COMBINE): oxic layer (C:P ratio ~ $[O_2]$) and constant sulfate reduction zone; Goddéris and Joachimski (2004)
MoBidiC	3 zonally averaged basins, 5° (meridional), 19 vertical layers	Fully coupled carbon-cycle, PO_4 limiting nutrient, Michaelis-Menten kinetics, Crucifix, (2005)	DIC, $DI^{13}C$, DOC, $DO^{13}C$, ALK, PO_4,O_2, ^{14}C, POC, $CaCO_3$	Single exponential	No sediment representation
Bern 2.5D	zonally averaged, 3-basin circulation model, 14 vertical layers Marchal et al. (1998)	Michaelis-Menten kinetics, PO_4 limiting nutrient and relation to temperature. Marchal et al. (1999)	DOC, DIC, C, $\delta^{13}C$, $\delta^{14}C$, PO_4, ALK, O_2, $CaCO_3$; Marchal et al. (1998b)	Power law (Martin)	No sediment representation

Glossary				
	3D resolution higher 10°x10°	Ecological model	Double exponential / Temp dependent	Vertically integrated, organic and inorganic carbon burial
	3D resoltion lower 10°x10°	Export production model (10 or more tracers)	Power law or single exponential	Vertically integrated inorganic carbon burial - no organic carbon burial
	zonally averaged basins or boxes	Export production model (less than 10 tracers) or simpler model	Linear/complete recycling	Constant preservation

Table 3: Overview of Earth system box models mentioned in this study and their characteristics related to the biological pump (Glossary of Table 2 applies here as well).

Models	Ocean Model Resolution	Ocean Carbon Cycle Surface Production	Tracers	Degradation	Sediments
Lower order ESM					
DCESS	2 x 55 boxes, 1 hemisphere, 100m vertical resolution, Shaffer et al. 2008	Export production model, PO4 limiting nutrient, Yamanaka and Tajika (1996)	POC, PO_4, O_2, DIC, ALK, $^{12,13,14}C$, $CaCO_3$	Single exponential	Semi-analytical, oxic respiration and denitrification, $CaCO_3$, Shaffer et al. 2008
SUE	Uses set-up of Bern 2.5D or PANDORA model	Export production model (siliceous and non-siliceous phytoplankton), limiting nutrients (PO_4, H_4SiO_4, Fe); Ridgwell (2001)	PO_4, H_4SiO_4, Fe, DIC, ALK, O_2, $CaCO_3$, POC, opal, DOM, $^{12,13}C$, $^{16,17,18}O$	Single exponential	$CaCO_3$ and opal as fct. of saturation state, Ridgwell et al. (2002), Archer (1991)
CYCLOPS	14/13 homogeneous boxes, e.g. Keir 1988, 1990; later 18 boxes, Hain et al. 2010	Fixed fraction of PO_4 depending on latitude, Keir (1988)	PO_4, O_2, DIC, ALK, $\delta^{13}C$, $\delta^{14}C$, POC, $CaCO_3$	Fixed fraction depending on latitude	1. Similar to LOSCAR (but const. porosity); 2. Respiration driven $CaCO_3$ dissolution, Sigman et al. (1996)
PANDORA	10/11 homogeneous boxes, e.g. Broecker and Peng (1986, 1987)	Limiting nutrients (PO_4, NO_3) with diff. residence times per box	PO_4, NO_3, O_2, DIC, ALK, $\delta^{13}C$, $\delta^{14}C$, POC, silica, $CaCO_3$, ^{39}Ar, ^3He, $^{13}C/^{12}C$	OM entirely recycled in water column	No sediment representation
LOSCAR	10 homogeneous boxes for modern ocean (13 e.g. for the P/E-version)	Biological uptake using Michaelis-Menten kinetics, PO_4 limiting nutrient	TCO_2, TA, PO_4, O_2, $\delta^{13}C$, pH, Mg/Ca	no organic carbon	%$CaCO_3$ in the bioturbated layer as a fct. of sediment rain, dissolution, burial and chemical erosion - also variable porosity
BICYCLE	10 homogeneous boxes (5 surface, 2 intermediate, 3, deep); Köhler et al. (2005)	Fixed fraction of PO_4, Munhoven and François (1996)	PIC, POC, PO_4, O_2, DIC, ALK, $\delta^{13}C$, $\delta^{14}C$	OM entirely recycled in water column	No sediment representation or restoration of prescribed lysocline or $[CO_3^{2-}]$
MBM	10 homogeneous boxes (5 surface, 2 intermediate, 3, deep)	Similar to BICYCLE	DIC, TA, PO_4, O_2, CO_2, $\delta^{13}C$,$\delta^{14}C$, OM, calcite, aragonite	Power law (Martin)	Advection-diffusion-reaction model MEDUSA: solids (clay, calcite, aragonite, OM), solutes (CO_2, HCO_3, CO_3, O_2)

285 we limit our review to carbon containing compounds and refer the interested reader to **?** and **?** for reviews on the ocean silica cycle.

3.1 Biological production

Biological production is controlled by the availability of light, nutrients, and trace metals, as well as phytoplankton speciation, temperature, and grazing. At steady state, nutrients removed from surface
290 waters in the form of descending particulate matter are balanced by the upward advective and diffusive supply of dissolved nutrients that support new production in surface waters (**?**). The production of PIC, POC and DOC in the surface ocean is thus driven by complex recycling and transformation pathways within the euphotic ecosystem (e.g. **?**). High data requirements, excessive computational demands, as well as the limited transferability of existing comprehensive ecosystem model ap-
295 proaches to the geological timescale compromise the application of these models in a paleo-context.

Export Production Models

Najjar et al. (1992); Maier-Reimer (1993); Yamanaka and Tajika (1996):

$$F_{\mathrm{POC}}(z) = (1-\delta)\cdot\int_0^{z_{\mathrm{eup}}} k_{\max}\cdot(NU-NU^*)dz \qquad \text{if} \quad NU > NU^* \tag{1}$$

$$F_{\mathrm{POC}}(z) = 0 \qquad \text{if} \quad NU \leq NU^*$$

or

$$F_{\mathrm{TOC}}(z) = \int_0^{z_{\mathrm{eup}}} k_{\max}\cdot\frac{NU}{NU+K_{\mathrm{NU}}}dz \tag{2}$$

$$F_{\mathrm{POC}}(z) = (1-\delta)\cdot F_{\mathrm{TOC}}(z) \tag{3}$$

$$F_{\mathrm{DOC}}(z) = \delta\cdot F_{\mathrm{TOC}}(z) \tag{4}$$

$$F_{\mathrm{PIC}}(z) = r_{\mathrm{PIC/POC}}\cdot F_{\mathrm{POC}}(z) \tag{5}$$

Biological Models

Mouchet and Francois (1996):

$$F_{\mathrm{POC}}(z) = \int_0^{z_{\mathrm{eup}}}\left(g_{\max}\cdot\frac{P}{P+K_{\mathrm{P}}}+d_{\mathrm{Ph}}\right)dz \tag{6}$$

$$F_{\mathrm{DOC}}(z) = 0$$

$$F_{\mathrm{PIC}}(z) = r_{\mathrm{PIC/POC}}\cdot F_{\mathrm{POC}}(z) \tag{7}$$

Six and Maier-Reimer (1996) (or similarly Schmittner et al., 2005):

$$F_{\mathrm{POC}}(z) = \int_0^{z_{\mathrm{eup}}}\left((1-\varepsilon_{\mathrm{her}})G\frac{P-P_{\min}}{P+P_0}Z + d_{\mathrm{Ph}}(P-P_{\min}) + (1-\varepsilon_{\mathrm{can}})d_{\mathrm{Zo}}(Z-Z_{\min})\right)dz \tag{8}$$

$$F_{\mathrm{DOC}}(z) = \int_0^{z_{\mathrm{eup}}}(\gamma_P(P-P_{\min})+\gamma_Z(Z-Z_{\min}))\,dz \tag{9}$$

$$F_{\mathrm{PIC}}(z) = r_{\mathrm{PIC/POC}}\cdot F_{\mathrm{POC}}(z) \tag{10}$$

Glossary

z	Water depth	z_{eup}	Bottom of euphotic zone
F_{A}	Flux of A	TOC	Total Organic Carbon
δ	Fraction of produced DOC	$k_{\max}$	Max. production rate
NU	Simulated nutrient concent.	NU^*	Fixed nutrient concentration
K_{NU}, K_P	Michaelis-Menten term	$r_{\mathrm{PIC/POC}}$	Rain ratio
$g_{\max}$	Max. grazing rate	d_{Ph}, d_{Zo}	Specific mortality rate
$(1-\varepsilon_{\mathrm{her}})$	Egestion as fecal pellets from herbivores	$(1-\varepsilon_{\mathrm{can}})$	Egestion as fecal pellets from carnivores
G	Available biomass	$P_{(\min)}$	(Min) phytoplankton concentration
P_0	Half-saturation concentration for phytoplankton ingestion		
$Z_{(\min)}$	(Min) zooplankton concentration	γ_P, γ_Z	Excretion rate of DOC

Figure 5: Overview of model approaches that are applied in paleoclimate models to calculate surface ocean production/export production.

Therefore, paleoclimate models generally treat surface ocean biogeochemical dynamics in a simplified way (see Fig. 5 for an overview).

3.1.1 Organic carbon production

Model approaches can be broadly divided into two different classes (Fig. 5). A first class of models simply relates the whole-community export production directly to the availability of nutrients within the euphotic zone using either a nutrient restoration scheme towards a fixed concentration distribution (NU^*, e.g. **?**), or a Michaelis-Menten term for uptake kinetics (e.g. **?**). These export production models sometimes account for the more refractory DOC pools by assuming that a fixed fraction, δ, of the produced carbon is converted to DOC in the production zone. The second class of models explicitly resolves, although in a very reduced and simplified way, part of the biological complexity that drives carbon production in the euphotic zone (**???**). In these models, the export production is driven by a pool of phytoplankton whose growth is controlled by the availability of nutrients, light, as well as temperature. Upon death, organisms feed the fast sinking particulate organic carbon pool and POC export production is thus determined by grazing and mortality rates. The biological model of **?** applies a simple maximum grazing rate with a Michaelis-Menten term that allows for a non-linear closure of the system. **?** on the other hand explicitly resolve the dynamics of nutrients, phytoplankton, zooplankton and detritus (NPZD-model) in the euphotic layer and account for the production of fecal pellets by both carnivors and herbivores. Furthermore, their model assumes that DOC is produced by exudation from phytoplankton and zooplankton excretion.

All Earth system box models integrate a simple export production model including highly parametrised maximum production terms, since their low spatial resolution does not permit the resolution of latitudinal temperature and light variations. Some EMICs also apply simple export production models, however, the maximum export production depends here on the ambient temperature and/or light conditions. The UVic model, CLIMBER-2 and LOVECLIM have more complex biological schemes, following **?**, **?** and **?**, respectively. Although there is still a controversy about nitrogen or phosphorus being the ultimate limiter of oceanic primary production at geological timescales (**???**), most paleoclimate models estimate export production directly from available surface phosphate concentrations, implicitly assuming that nitrogen fixation compensates for a potential nitrogen limitation.

Box 1: Calcium carbonate thermodynamics primer

One of the most common minerals on Earth is calcium carbonate ($CaCO_3$) which is almost exclusively formed by biological processes. In the ocean $CaCO_3$ most commonly exists in two crystal forms: *calcite* and *aragonite*. Because calcite is the more thermodynamically stable phase it is more abundant in the ocean and forms almost all deep sea carbonate sediments. Aragonite, on the other hand, is found in shallow-water sediments (e.g. corals). Carbonate precipitation can be described by the following chemical reaction:

$$Ca^{2+} + 2HCO_3^- \rightarrow CaCO_3 + CO_{2(aq)} + H_2O$$

Whether $CaCO_3$ precipitates or dissolves can be directly linked to the concentrations of Ca^{2+} and CO_3^{2-} in sea-water which controls the stability of its crystal structure (**?**). This is expressed as the *saturation state* Ω of the solution and is defined as

$$\Omega = [Ca^{2+}] \times [CO_3^{2-}]/K_{sp},$$

where K_{sp} is a solubility constant which scales with increasing pressure (**?**). Calcium carbonate is thermodynamically favourable to precipitate at $\Omega > 1$ (i.e. in oversaturated environments) and prone to dissolution when Ω is smaller than unity. The saturation state of the ocean generally decreases with water depth in response to the combined effects of the pressure-induced increase in the solubility constant and the release of CO_2 through the degradation of sinking POC that decreases the ambient pH and thus the carbonate ion concentration (**??**). Oceanic waters become undersaturated (i.e. $\Omega < 1$) below the depth of the *saturation horizon* (i.e. $\Omega = 1$) and carbonates start to dissolve. However, the process of dissolution proceeds only extremely slowly in the beginning. The depth at which the dissolution rate increases considerably and impacts become noticeable is known as the *lysocline* (**?**) (sometimes defined at $\Omega = 0.8$, **?**). Deeper still, the rate of dissolution becomes fast enough to exactly balance the rate of supply of carbonates to the sediments and therefore no carbonates are preserved. This is termed the *carbonate compensation depth* (CCD) (compare Fig. 2).

3.1.2 Pelagic calcium carbonate production

Today, the surface ocean is largely oversaturated with respect to carbonate phases (see Box 1 for a carbonate primer; **?**). Nevertheless, due to the kinetically unfavourable initial step of crystal nucleation, abiotic carbonate precipitation is rare and only occurs in extreme environments as cements or ooids (e.g. **??**). In the open ocean, the most important groups for the production of calcium carbonate ($CaCO_3$) are marine organisms like coccolithophores, foraminifera and pteropods. These three groups are responsible for up to 70% of global $CaCO_3$ precipitation (**?**). Coccolithophores are a group of algae (mostly unicellular) that form an outer sphere of small calcite crystals, known as coccoliths. The other two groups are heterotrophic zooplankton. Foraminifera form skeletons made out of calcite and pteropods, a general term for a group of molluscs, produce crystals made out of aragonite (the thermodynamically less stable form of calcium carbonate).

As these biological processes and their links to ocean geochemistry are very complex, most paleoclimate models calculate marine carbonate export production as a fixed fraction of POC export production (the $r_{\mathrm{PIC/POC}}$ "rain ratio", compare Fig. 5 and e.g. **?**). However, there is no simple means of deriving the value of $r_{\mathrm{PIC/POC}}$ as it is highly dependent on the local ecosystem structure (**?**). Paleoclimate models that integrate biological models generally apply a formulation that relates the rain ratio to the ecosystem structure. Otherwise, highly parametrised formulations on the basis of ambient temperature conditions (e.g. **????**) or the saturation state with respect to calcite are used (**??**). Only a small number of paleoclimate models distinguish between calcite and aragonite fractions as most of the global PIC export is driven by low-Mg calcite from coccolithophores and foraminifera (**??**). The aragonite cycle is still poorly quantified and therefore, its rain ratio is considered in a few models only: LOCH/LOVECLIM (**?**), MBM (**??**), and optionally in Bern 3D (**?**). Estimates for the fraction of aragonitic pteropods or heteropods in the global ocean carbonate rain are in the range of 10–50% (**???**).

3.2 Intermediate and deep ocean

The remineralisation of biogenic particles exported from the surface ocean redistributes carbon and nutrients in the ocean exerting an important influence on atmospheric $\mathrm{CO_2}$ levels. Changes in the depth-distribution of POC remineralisation controls the sequestration of $\mathrm{CO_2}$ in the water column on timescales of decades to centuries (**?**) whereas changes in the ratio of POC to $\mathrm{CaCO_3}$ in fluxes reaching the sediment may change $\mathrm{CO_2}$ over thousands to millions of years (**??**). However, despite considerable effort to identify potential processes that control the fate of organic carbon in water column (e.g., Joint Global Ocean Flux Study (JGOFS, **?**); VERtical Transport In the Global Ocean (VERTIGO, **?**)), the key processes are still not well understood (**?**).

3.2.1 Particulate Organic Carbon

3.2.1.1 Observations

Field observations across the global ocean show that a large fraction of particulate organic carbon is efficiently degraded by bacterial activity as it sinks through the water column and that the recycling process is exponentially faster in the mesopelagic layers of the ocean than in the deeper ocean (e.g. **???**, compare Fig. 2 and 7). This is generally explained with either increasing particle sinking speeds with depths (**?**) or a decrease in organic matter reactivity with depth/age because as POC sinks, labile

organic components are degraded more readily, leaving more refractory material behind (e.g. **?**). However, the overall importance of this so-called selective preservation remains disputed (e.g. **??**), and little is known about the mechanistic control on decreasing organic matter degradability during sinking. Other mechanisms, such as physical protection (e.g. **?**) likely also contribute to decreasing organic matter reactivity. Compilations of globally distributed sediment trap data show that the rate of attenuation with depth varies generally with latitude. However, very little is known about what controls this geographical variability and different observations are seemingly inconsistent (see e.g. **??**). Various mechanisms have been postulated to explain these spatial patterns, focusing again on either changes in the sinking rate or the degradation rate of POC.

As the density of typical organic matter ($\sim$1.05 g cm^{-3}, **?**) is close to that of seawater ($\sim$1.02–1.03 g/cm^{-3}) POC needs to aggregate or a source of weight in order to contribute significantly to the organic matter flux to the deep ocean. Strong global correlations between inorganic minerals (such as $CaCO_3$, opal and lithogenic material) and POC fluxes in the deep ocean led to the hypothesis that the denser minerals increased the density, and therefore sinking rate, of POC (the "ballast hypothesis") (**??**). Deep ocean POC fluxes are thus driven by the local biomineral (i.e. high in calcite-dominated and low in opal-dominated regions.) However, analyses of these relationships on temporal (**?**) and spatial scales (**?**) have questioned the relative role of minerals as ballast material. The correlations may also reflect other processes governing the association between POC and minerals such as the presence of transparent exopolymer particles (TEP) that stimulate aggregation **??**. Another explanation for the observed regional POC flux variability is a temperature dependence for the degradation of organic matter. Temperature is a primary determinant for bacterial degradation rates (**??**) and it has been shown that degradation rates are more sensitive to temperature than photosynthesis (**??**). Thus, warmer waters are characterised by faster degradation rates and therefore shallower remineralisation (**?**).

A hypothesis that combines elements of the previous mechanisms specifies ecosystem structure and specifically the extent of recycling of organic matter in the euphotic zone as an important factor governing the observed spatial variability in POC flux (**???**). The reasoning is that in high export production areas (generally colder high latitudes) aggregates are rather fresh and loosely packed as they are a result of strong, seasonal diatom blooms, making them prone to rapid degradation. In low export production areas (warmer low latitudes) the material being finally exported has been

processed multiple times in the euphotic layer and is therefore tightly-packed, highly refractory and thus experiences reduced microbial degradation at mesopelagic depths (**?**).

An increasing number of mechanisms have been identified that may contribute to changes in the attenuation of POC flux in the water column. However, as highlighted above, these mechanisms are potentially interlinked and difficult to distinguish from current observations. This represents a significant source of uncertainty surrounding the magnitude and sign of ocean carbon cycle feedbacks to changes in atmospheric CO_2 and climate (**??**).

3.2.1.2 Numerical approaches

Most Earth system models impose static POC depth profiles and are therefore based on simple fitting exercises to limited data sets rather than on a mechanistic understanding of the underlying processes. This is surprising, since more sophisticated models have long been used to study organic carbon degradation dynamics in soils and marine sediments over different timescales (e.g. **?**). Even though still far from providing an appropriate representation of the plethora of different mechanisms that control organic carbon degradation, these models have proven useful in describing the degradation dynamics of organic carbon from different sources, in different environments, under changing redox-conditions and over timescales (e.g. **?**). The applied approaches in ocean biogeochemical models can be broadly divided into two groups: the primarily empirical approaches and more mechanistic approaches of various levels of complexity.

In the early 1980's net primary productivity (NPP) in the surface waters was assumed to be most important for vertical POC flux. The empirical algorithm of **?** (equation (1) in Fig. 6) describes POC flux to depth as a function of NPP, scaled to depth below the sea-surface. However, **?** demonstrated that export (or new) production of POC (i.e. POC exported from the euphotic zone) predicts POC flux in deeper waters more reliably and is used until now in biogeochemical models. Other empirically derived relationships used in paleoclimate models are intentionally or unintentionally related to more mechanistic descriptions of organic carbon degradation. Power-law (**?**), single exponential (**???**) or double exponential (**??**) relationships are applied in most of the paleoclimate models (Table 2). Although these models are usually empirical as well, they can be directly derived from the kinetic first-order rate law of organic matter degradation:

$$\frac{d\mathrm{POC}}{dt} = k \cdot \mathrm{POC}. \tag{1}$$

Suess Model

Suess (1980):

$$F_{\mathrm{POC}}(z) = \frac{C_{\mathrm{NPP}}}{0.0238 \cdot z + 0.212} \tag{1}$$

Single Exponential Model

e.g., Heinze et al. (1999)

$$F_{\mathrm{POC}}(z) = F_{\mathrm{POC}}(z_{\mathrm{eup}}) \cdot \exp\left(-\frac{z - z_{\mathrm{eup}}}{L_{\mathrm{POC}}}\right) = F_{\mathrm{POC}}(z_{\mathrm{eup}}) \cdot \exp\left(-\frac{k}{w}(z - z_{\mathrm{eup}})\right) \tag{2}$$

Martin Model

Martin et al. (1987):

$$F_{\mathrm{POC}}(z) = F_{\mathrm{POC}}(z_{\mathrm{eup}}) \cdot \left(\frac{z}{z_{\mathrm{eup}}}\right)^{-b} \tag{3}$$

Double Exponential Model

e.g., Lutz et al. (2002) or Andersson et al. (2004):

$$F_{\mathrm{POC}}(z) = f \cdot F_{\mathrm{POC}}(z_{\mathrm{eup}}) \cdot \exp\left(-\frac{k_1}{w_1}(z - z_{\mathrm{eup}})\right) + (1 - f) \cdot F_{\mathrm{POC}}(z_{\mathrm{eup}}) \cdot \exp\left(-\frac{k_2}{w_2}(z - z_{\mathrm{eup}})\right) \tag{4}$$

Reactive Continuum Model

Boudreau and Ruddick (1991):

$$F_{\mathrm{POC}}(z) = F_{\mathrm{POC}}(z_{\mathrm{eup}}) \cdot \left(\frac{a}{a + (z - z_{\mathrm{eup}})/w}\right)^{u} \tag{5}$$

Glossary

z	Water depth	z_{eup}	Bottom of euphotic zone
F_{POC}	Flux of POC	C_{NPP}	NPP of organic matter in surface
b	Flux attenuation factor	L_{POC}	POC degradation length scale
k_i	Degradation rate of POC	w_i	Sinking rate of POC
f	Labile fraction of POC	a	Average life-time of labile POC
u	Non-dimensional parameter		

Figure 6: Overview of model approaches that are applied in paleoclimate models to calculate the depth profiles of POC fluxes in the water column.

and the chosen function reflects certain assumptions about the organic matter pool and its degradation rate k. Therefore, the representation may be more directly related to some underlying bioenergetic drivers (**??**). The rate constant of organic carbon degradation, k, is usually interpreted as a measure of the reactivity of the macromolecular organic matter towards hydrolytic enzymes and is thus assumed to primarily depend on the macromolecular composition of organic matter. It therefore encompasses not only the original composition of the exported organic carbon, but also its evolution during sinking (**?**). The simplest form of this approach assumes that the organic carbon constitutes one single pool, which is degraded at a constant rate. This approach is equivalent to the so-called 1G-Model of organic matter degradation (**?**) that has been widely used in diagenetic modelling (**?**). Its steady-state solution is given by a simple exponential decrease of organic carbon flux with depth that is controlled by the reactivity of organic carbon, k, and the settling velocity, w (equation (2) in Fig. 6; see **?** for a derivation). Yet, this simple exponential model represents merely a linear approximation of the complex degradation dynamics and the first-order degradation constant, k, represents a mean value for the heterogeneous mixture of organic compounds. It should be noted that such simplification is reasonable only if the degradability of different compounds does not vary by more than one order of magnitude (**?**).

Under the assumption that the organic carbon degradation rate decreases linearly with depth, a power-law functionality for POC flux can be derived from kinetic first-order principles (compare supporting information of **?**). Most commonly used is the description of (**?**) – equation (3) in Fig. 6. **?** fitted a number of sediment trap POC flux measurements from six different locations in the northeast Pacific Ocean to a simple power-law. The expression scales deep fluxes to POC export from the euphotic zone (z_{eup}) and flux attenuation with depth is parametrised with a constant parameter $b = 0.858 \pm 0.1$. The majority of existing paleoclimate models integrate the Martin curve in its original form with a constant parameter b (Table 2) that does not change temporally or spatially. Its popularity mainly stems from the fact that a power-law represents a mathematically simple way to describe the sharp decrease of organic carbon fluxes in mesopelagic layers, while still maintaining a flux at depth.

Yet, in reality, the organic carbon flux to depth is composed of many specific and very heterogeneous compounds with a continuum of individual decay rates, distributed from very labile compounds that are degraded within several hours or days to highly condensed compounds that persist for hundreds of thousands or even millions of years. The assumption of a single organic carbon pool that is degraded with a constant or linear degradation rate is thus not consistent with natural

conditions. The bulk POC flux can be subdivided into a number of compound classes that are characterised by different degradabilities k_i. This approach follows the multi-G approach proposed by **?** and **?** to describe organic carbon degradation in marine sediments. The rapid depletion of the more reactive compound class results in a decrease of total organic carbon degradability with water depth and therefore provides a more realistic representation of organic carbon degradation dynamics (**??**). **?** propose to describe organic carbon flux to depth using a double exponential equation including degradation length scales for a labile and a refractory fraction of POC (equation (4) in Fig. 6). For instance GENIE integrates such a double exponential expression that can capture the rapid flux attenuation in subsurface waters as well as the slower flux attenuation in deep waters. In theory, this 2G-Model could be expanded by introducing other POC compound classes, but as they are difficult to identify from observational data their number is generally restricted to three (**??**). An alternative to these models are Reactive Continuum Models (RCMs) of organic matter degradation (equation (5) in Fig. 6). These models assume a continuous distribution of reactive types, thus avoiding the highly subjective partitioning of POC into a limited number of compound groups (e.g. **??**). A newer version of GEOCLIM (GEOCLIM *reloaded*; **?**) applies the RCM to quantify POC fluxes below the euphotic zone. The RCM provides a direct conceptual link between the composition of organic matter and its degradability. The total amount of organic matter is represented as the integral of the distribution function of reactive types over the entire range of possible degradation rate constants. Each member is degraded according to a first order rate law. The RCM thus explicitly integrates the effect of compound-specific reactivities on organic matter degradation and captures the decrease in organic matter degradability with depth/age. However, the RCM approach requires the determination of realistic differential reactivities of specific components rather than an average reactivity for the total POC pool which can be challenging.

3.2.1.3 Comparing numerical approaches

Fig. 7 compares some of the discussed approaches with a compilation of globally distributed POC flux observations from the modern day (**?**). The Henson-approach uses the Martin equation but calculates the b-value in relation to local SST ($b = (0.024 \cdot SST) - 1.06$, compare **?**, Fig. 4f). A mean SST of 17.4 °C leads to a global mean b-value of -0.643 and therefore predicts higher residual POC flux in the deep ocean as the Martin model, showing how sensitive this approach is to changing b-values. The ballasting-method assumes that part of the POC export is associated with a ballasting

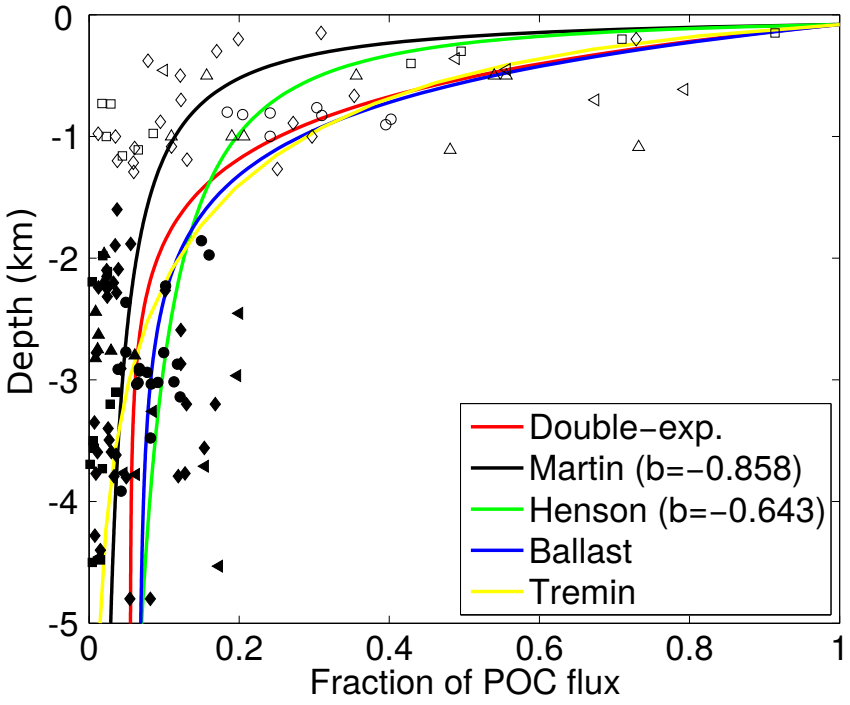

Figure 7: Comparison of discussed POC flux representations and global POC flux data from **?**. Observations shallower than 1.5 km have been divided by 0.4 to account for the potential undertrapping error (open symbols). Observations: ■/□: Atlantic Ocean, ♦/♢: Pacific Ocean, •/○: Indian Ocean, ▲/△: Greenland Sea. POC flux data has been normalised to regional POC export estimates given in **?** - Table 2.

mineral (here calcium carbonate) and the excess POC is considered the labile fraction (**??**):

$$F_{\mathrm{POC}}(z) = \lambda_{\mathrm{Ca}} \cdot F_{\mathrm{Ca}}(z) + F_{\mathrm{labile}}(z), \tag{2}$$

where $F_{\mathrm{POC}}(z)$ is the total POC flux at depth z, $\lambda_{\mathrm{Ca}} = 0.126$ the carrying coefficient of $\mathrm{CaCO_3}$, $F_{\mathrm{Ca}}(z)$ and $F_{\mathrm{labile}}(z)$ the total calcium carbonate and labile POC mass flux as calculated with GENIE. The temperature dependent remineralisation follows the description of **?** using an Arrhenius-type equation to predict the temperature dependent remineralisation rate $k(T)$:

$$k(T) = A \cdot \exp(-\frac{E_{\mathrm{a}}}{RT}), \tag{3}$$

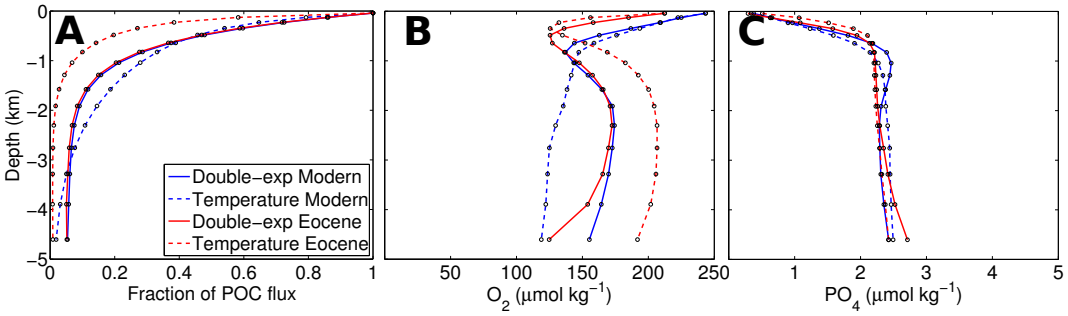

Figure 8: Modern and Eocene global profiles for a GENIE set-up using a double-exponential and temperature-dependent POC remineralisation approach. See Box 2 for more information about the experiment set-up.

where R is the gas constant and T the absolute temperature. To distinguish between labile and refractory POC two activation energies E_a (55 and 80 kJ mol^{-1}, resp.) and two rate constants A (9×10^{11} and 1×10^{14} year^{-1}, resp.) were chosen (as calibrated in **?**). The mean temperature profile for the global ocean has been taken from the World Ocean Atlas (**?**). In principle, all shown formulations are able to capture the characteristic POC-flux profiles for the modern day ocean (Fig. 7). However, as the parameters applied in paleoclimate models are constrained to modern-day observations (e.g. **??**) and the performance of the models strongly depend on the parameter choice, their predictive ability under different climatic conditions is seriously compromised.

To illustrate the impact of using a static versus a mechanistic POC-flux representations on ocean biogeochemistry we compare the fixed double-exponential with the temperature-dependent remineralisation approach using the paleoclimate model GENIE (see Box 2 for more information on the model and experiment set-up). Fig. 8 compares global POC, oxygen and nutrient profiles for a modern and a warm Eocene (55.5–33.7 Ma) climate. The global POC flux profile (normalised to export flux) for the static double-exponential just changes slightly in the Eocene experiment, whereas the temperature-dependent profile gets significantly shallower and a smaller POC fraction reaches the sediments due to warmer ocean temperatures (Fig. 8A). The global O_2 profile for the temperature-dependent parametrisation in the Eocene also shows this shoaling compared with the modern (Fig. 8B). But the temperature dependence of POC remineralisation has also major impacts on the modern ocean as can be inferred from the global O_2 profile, showing a different shape compared with the double-exponential scenario. However, in contrast the global profiles for PO_4 do not change significantly (Fig. 8C), a result that can be attributed to the fixed initial global phos-

Box 2: The paleoclimate model GENIE and the experiment set-up

The "Grid ENabled Integrated Earth system model" (GENIE)

The basis GENIE is a 3D-ocean circulation model coupled to a fast energy-moisture balance 2D-atmosphere model ("C-GOLDSTEIN", **?**). To help understand the oceanic carbon cycle and its role in regulating atmospheric CO_2 concentrations the model has been extended with a ocean biogeochemistry representation for a variety of elements and isotopes (**?**). The ocean model is implemented on a 36×36 equal-area horizontal grid and 16 z-coordinate levels in the vertical. Despite its lower resolution, GENIE is able to reproduce the main nutrient and dissolved inorganic carbon $\delta^{13}C$ features of the modern ocean (**??**). The same model physics have been applied before to an early Eocene and late Cretaceous bathymetry and continental configuration and successfully modelled various oceanic and sedimentary properties related to the biological carbon pump (**????**).

Experiment set-up: Oceanic POC-flux representations (Fig. 8, 9 and 10)

The GENIE set-up for the modern and Eocene experiments is identical to **?**. The OAE2 experiments adopt the carbon cycle boundary conditions of **?** using 2 times modern oceanic phosphate concentration (4.5 μmol PO_4 kg^{-1}) and 4 times preindustrial atmospheric CO_2 (1112 ppmv). However, we do not consider nitrogen in our simulations, thus phosphate being the only productivity limiting nutrient. All experiments are run for 10,000 years in order to equilibrate the ocean biogeochemistry. In the reference model set-up, POC-flux throughout the water-column is modelled using the fixed double-exponential approach (equation (4), Fig. 6). The temperature-dependent remineralisation uses the formulation as discussed for Fig. 7. The free parameters of this approach (i.e. two rate constants (A) and the initial refractory fraction of POC) were calibrated for the modern ocean to find the best fit with the double-exponential approach for the global POC-flux profile. The two approaches are then used under a preindustrial (modern) configuration (**?**), an early Eocene set-up (**?**) and an OAE2 configuration (**?**).

Experiment set-up: Sediment representations (Fig. 16 and 17)

For this series of experiments GENIE employs the fixed double-exponential POC-flux scheme but is configured with two different sediment boundaries for the modern, Eocene and OAE2 worlds: First, the so-called reflective boundary, where essentially no sediment interactions take place and all particulate species reaching the seafloor are instantaneously remineralised to dissolved carbon and nutrients. The second boundary represents the other end of the spectrum and assumes that the entire deposition flux of POC is buried in the sediments (conservative or semi-reflective boundary). In order to calculate a steady-state situation we configure the model as a "closed" system where the burial loss to the sediments is balanced by an additional weathering input of solutes to the ocean through rivers. Because of the sediment interactions the experiments are run for 20,000 years to reach equilibrium.

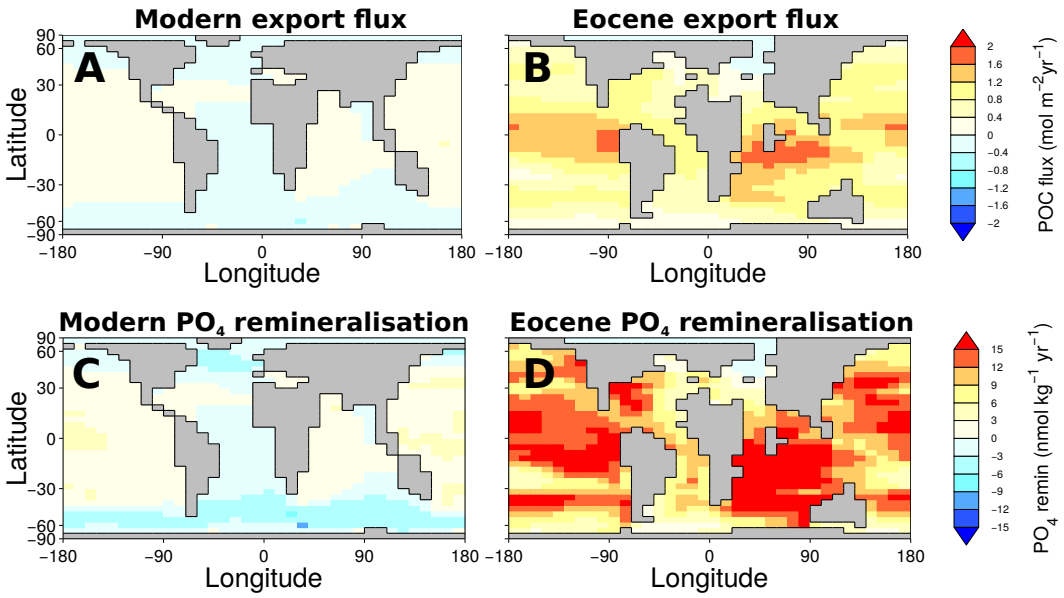

Figure 9: Anomaly plots (temperature-dependent minus double-exponential POC remineralisation approach) for the modern (left panel) and the Eocene (right panel). Top: Export production (i.e. POC flux at 40m). Bottom: Depth integrated remineralisation concentration of PO_4.

phate inventory imposed onto the model (compare also, e.g., **?**). The POC remineralisation scheme has not just significant impacts on global mean biogeochemical values but also affects their spatial distribution. Fig. 9 shows anomaly plots (temperature-dependent minus double-exponential) for export production (A and B) and depth integrated remineralisation concentrations of PO_4 (C and D). The differences for modern conditions are marginal (Fig. 9, A and C) as the temperature-dependent POC flux has been calibrated to the double-exponential flux for these conditions. However, for the Eocene, the temperature-dependent export production increases globally (9.6 Pg C year^{-1} compared to 5.9 Pg C year^{-1} in the double-exponential simulation), in particular in warm equatorial regions (Fig. 9B). Also the depth integrated PO_4 remineralisation is significantly higher (Fig. 9D). Both can be explained by the shallower, temperature dependent degradation of POC in the warmer Eocene, leading to higher PO_4 availability in the upper ocean and therefore an absolute increase in global productivity.

Fig. 10 compares the two remineralisation approaches for another extreme event in Earth history, the Late Cretaceous oceanic anoxic event (OAE2). Shown are modelled H_2S concentrations, another indicator for ocean redox conditions, for the two GENIE configurations for OAE2. Euxinia is defined

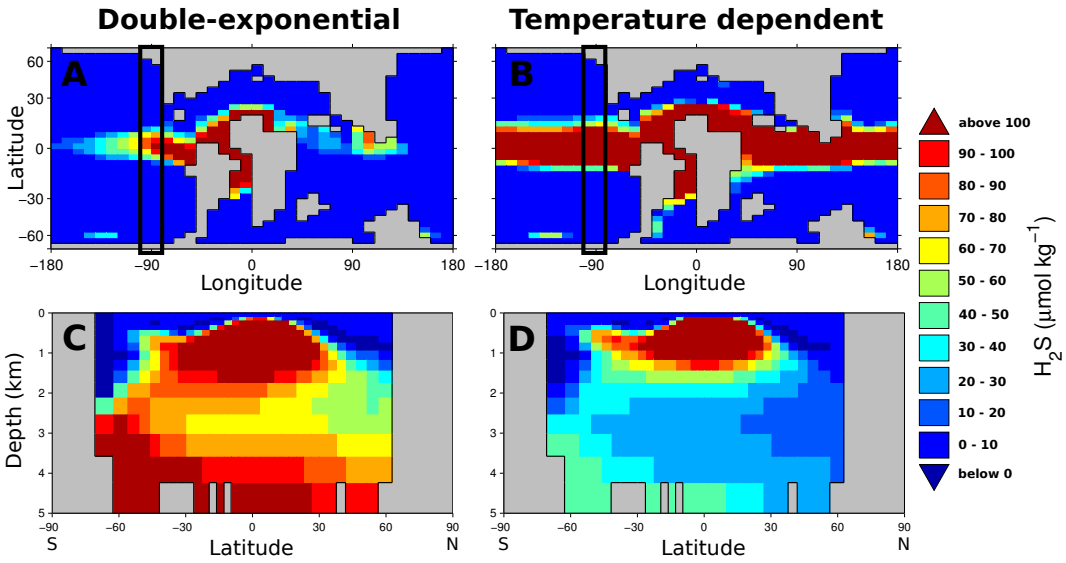

Figure 10: Model comparison of H_2S concentration (i.e. euxinia) during OAE2 for a GENIE configuration with double-exponential (left) and temperature-dependent (right) POC remineralisation approach. (A+B): Photic zone euxinia showing modelled H_2S concentration at 80-200 m. (C+D): Vertical profile of H_2S in the East Pacific Ocean ($-90°$ longitude, area indicated by black rectangles in A+B).

by the occurrence of free hydrogen sulfide in the water column, which is characteristic of anoxia as H_2S is produced by sulfate reduction when oxygen is depleted. Fig. 10A+B highlights the significant impact the POC-flux representation has on photic zone euxinia, with far more H_2S predicted when the temperature-dependent approach is used, a result that can be explained with warmer ocean temperatures leading to more POC degradation in the upper ocean (POC profile for OAE2 is similar to the Eocene Fig. 8, not shown here). However, as the majority of POC is degraded in the upper 500m when using the temperature-dependent approach, less H_2S is produced in the deeper ocean (Fig. 10C+D).

3.2.1.4 Summary

The different model results highlight that the current lack of a mechanistic theoretical framework to model POC flux seriously compromises the applicability of paleoclimate models to extreme and rapidly changing environmental conditions. A complex process interplay controls organic carbon degradation in the Earth system. It has been shown that the availability of oxygen, variable redox-

conditions, euxinic environmental conditions or changing organic carbon sources can exert profound impact on organic matter reactivity and thus degradation and burial (e.g. **?????**). A robust mechanistic framework is therefore a crucial prerequisite to increase the predictive ability of POC flux models, especially under changing environmental conditions that typically characterise past carbon-cycle perturbations.

3.2.2 Dissolved Organic Carbon

3.2.2.1 Observations

With a size of about 662 Pg C, marine dissolved organic carbon (DOC) is comparable to the amount of carbon in the atmosphere (**?**). Recently, various studies have re-emphasized the importance of DOC in the ocean and its contribution to the biological pump (e.g. **???**). Most marine DOC is produced (together with POC and PIC) by phytoplankton in the surface ocean and accounts for about 30–50% of the primary production (**??**). A large part of the produced DOC belongs to the labile or semi-labile DOC pool. The labile fraction is directly recycled in the euphotic zone (lifetime hours to days), whereas the semi-labile DOC mostly consists of carbohydrates that are degraded by heterotrophic processes in the upper 500 m of the ocean (see Table 4). Therefore, semi-labile DOC represents an important contributor to the biological carbon pump. Due to short lifetimes the labile and semi-labile DOC fractions account for a mere 1% of the total DOC inventory and have a limited importance for longer carbon sequestration (**?**). The remainder is transported further to deeper waters through the overturning circulation of the ocean or scavenging on sinking aggregates and can be broadly divided into a semi-refractory and refractory pool (**?**). Semi-refractory DOC is mainly found at mesopelagic depth of the ocean (< 1000 m) and accounts for about 2% of the DOC inventory (lifetime years to multiple decades, **?**). **?** argues that most of the deep ocean DOC is largely unreactive and degrades on timescales of several hundreds to thousands of years. This refractory DOC pool thus survives several cycles of ocean overturning and represents the largest fraction of the total marine DOC reservoir (about 97%, Table 4). Therefore, it is mostly argued that semi-labile DOC largely dominates the upper ocean (< 500 m), while semi-refractory and refractory DOC represents most of the DOC in the deep ocean (**?**). In contrast, **?** and **?** hypothesise that most of the deep ocean DOC is in fact labile but that its very low concentrations limit their microbial utilisation. This “dilution hypothesis” is supported by the fact that most of the refractory DOC is

Table 4: Characterisation of major DOC fractions (after **?**).

Fraction	Inventory (Pg C)	Removal rate (μmol C kg^{-1}year^{-1})	Lifetime	main occurance
Labile	<0.2	∼100	hours to days	directly recycled
Semi-labile	6±2	∼2–9	months to years	upper mesopelagic zone (< 500 m)
Semi-refractory	14±2	∼0.2–0.9	years to decades	mesopelagic zone (< 1000 m)
Refractory	642±32	∼0.003	centuries to millennia	everywhere

still unclassified (**?**) and little evidence exists to proof that it should not be available for microbial degradation.

3.2.2.2 Numerical approaches

Despite these uncertainties and its unquantified importance for the biological pump, none of the paleoclimate box models integrate an explicit description of DOC (Table 5). Most other models describe the heterotrophic degradation of just one single DOC pool by a first order degradation rate law:

$$\frac{\partial \mathrm{DOC}}{\partial t} = k_{\mathrm{DOC}} \cdot \mathrm{DOC}. \tag{4}$$

The Bern models, for instance, assume a constant oceanic DOC inventory (**?**). As a consequence, DOC is degraded with a first order degradation rate constant, k_{DOC}, that is dynamically adjusted in a way that DOC production in the euphotic zone is balanced by its degradation in the deep ocean. This approach has been first proposed by **?** who argue that the rate constant for DOC degradation cannot be constrained on the basis of data available at that time. The DOC lifetime in MoBidiC has been calibrated to 8.6 years, whereas LOVECLIM applies a degradation rate constant depending on oxygen availability resulting in a DOC lifetime between 20 and 22 years. Both models therefore capture the dynamics of the semi-refractory DOC pool. The standard setup of GENIE accounts for a semi-labile DOC fraction with a lifetime of 0.5 years. GENIE also has the option to represent a second DOC pool which has been used by **?** to model a semi-refractory and a refractory DOC pool (lifetimes of 20 and 10,000 years) for the last glacial maximum. Dissolved organic carbon in the CLIMBER family is simulated with the biological model of **?**. Therefore, the concentration of DOC depends on exudation from phytoplankton, excretion from zooplankton and a nutrient dependent

Table 5: DOC representation in paleoclimate EMICs. Note, none of the reviewed Earth system box models represents a DOC pool.

Model	DOC fraction	Lifetime	Reference
UVic	semi-labile/semi-refractory	2–6 years	**?**
LOVECLIM	semi-refractory	20–22 years	**?**
Bern 3D	constant inventory	dynamic	**?**
MESMO	semi-labile	0.5 years	**?**
GENIE	semi-labile	0.5 years	**?**
	semi-refractory	20 years	**?**
	refractory	10,000 years	**?**
CLIMBER-2	labile/semi-labile	days to 1 year	**?**
	semi-refractory	40 years	**?**
GEOCLIM	–	–	–
MoBidiC	semi-refractory	8.6 years	**?**
Bern 2.5D	constant inventory	dynamic	**?**

degradation constant (resulting in a lifetime between days and one year). The CLIMBER-2 model also provides the possibility to allocate 10% of the produced detritus to another, semi-refractory DOC pool with a lifetime of 40 years (**?**). Paleoclimate models thus mainly account for the cycling of, what is operationally classified as, the semi-labile and semi-refractory DOC fractions and generally ignore the largest DOC reservoir and its contribution to the biological carbon pump via carbon sequestration.

3.2.2.3 Summary

A more realistic representation of DOC in paleoclimate models should include several fractions of DOC with different lifetimes (**?**) and the advantages of using a reactive continuum model for DOC should be tested. The lack of a better representation of DOC is often attributed to the limited knowledge about the processes and mechanisms involved in the generation and degradation of this carbon reservoir (e.g. **?**). Yet, over the recent years, considerable progress has been made in advancing our understanding of the ocean's DOC reservoir (e.g. **?**). In addition, a number of authors have recently argued that especially the refractory DOC pool may have played a central role for past carbon isotope excursions and associated climate change (e.g. **??**). **?** suggested that an anoxic and stratified Eocene deep ocean may have facilitated the accumulation of a large refractory DOC reservoir. Periodic release and oxidation of this surficial carbon pool (about 1,600 Pg C) as a consequence of changes in ocean circulation could explain the observed rapid decline in the $\delta^{13}C$ record and as-

sociated climate warming. The rapid recovery of the global carbon cycle is for **?** an indicator that CO_2 was sequestered again by the ocean and not by the slower process of silicate rock weathering. However, one problem with this hypothesis is the unknown sensitivity of DOC degradation to ocean oxygenation (compare e.g. **?**). Elucidating the role of DOC in general and the refractory DOC pool in particular for past carbon cycle and climate perturbations will thus require a better integration of DOC in paleoclimate models.

3.2.3 Particulate Inorganic Carbon

3.2.3.1 Observations

The cycling of particulate inorganic carbon (i.e. $CaCO_3$) in the ocean also affects the biological pump and therefore atmospheric CO_2, but by more indirect mechanisms. Whether carbonates precipitate or dissolve can be directly linked to the saturation state (Ω) of the ocean (readers are referred to Box 1 for a brief primer on carbonate thermodynamics). Compared to the 5% of POC that is exported from the euphotic zone and reaching the sediments, a significantly higher amount of PIC is vertically transported to the bottom of the ocean (about 50% of the PIC export flux, **?**). The role of sinking particulate inorganic carbon in the biological pump is complex, because the deep dissolution of PIC is largely controlled by the degradation of sinking POC and releases alkalinity, which in turn titrates part of the CO_2 released during POC degradation. In addition its high specific gravity plays a key role for the sinking rates of biogenic aggregates (the ballasting effect) and thus the residence time of particulate carbon in the ocean (e.g., **??**). The mechanisms responsible for carbonate dissolution in the ocean are still matter of debate (**?**). Global observations showing that the depth of the lysocline coincides with the saturation horizon (e.g. **?**) have been used to imply that thermodynamic constraints are a dominant control on calcium carbonate preservation. However, a kinetic control on carbonate dissolution has been highlighted by in-situ experiments in the North Pacific (e.g., **?**) and laboratory studies reveal that dissolution rates increase in undersaturated waters (**??**). In addition, observational evidence even points to a partial dissolution of sinking carbonate above the saturation horizon (e.g. **?**). **?** estimates, using global production estimates of $CaCO_3$ and globally averaged deep water sediment trap data, that probably 40–80% of the calcium carbonate produced in the surface ocean dissolves in the upper water column. However, the mechanisms that drive the dissolution of carbonates above the lysocline remain enigmatic. The dissolution of carbonates within acidic micro-environments, such as the digestive system of zooplankton or marine aggregates have been

Exponential Model

(e.g., Maier-Reimer, 1993):

$$F_{\mathrm{PIC}}(z) = F_{\mathrm{PIC}}(z_{\mathrm{eup}}) \cdot \exp\left(-\frac{(z - z_{\mathrm{eup}})}{L_{\mathrm{PIC}}}\right) \qquad \text{for} \quad z_{\mathrm{eup}} < z \leq z_{max} \tag{1}$$

Thermodynamic Models

Vertically Resolved (e.g., Morse and Berner, 1972, Gehlen et al., 2007):

$$\frac{dF_{\mathrm{PIC}}(z)}{dz} = 0 \qquad \text{if} \quad \Omega \geq 1 \tag{2}$$

$$F_{\mathrm{PIC}}(z) = F_{\mathrm{PIC}}(z_{\mathrm{lys}}) \cdot \exp\left(-\frac{k_{\mathrm{PIC}}(1-\Omega)^n}{w}(z - z_{\mathrm{lys}})\right) \qquad \text{if} \quad \Omega < 1 \tag{3}$$

Simplified (Dissolution solely at the bottom of the ocean):

$$\frac{dF_{\mathrm{PIC}}(z)}{dz} = 0 \qquad \text{for} \quad z_{\mathrm{eup}} < z \leq z_{max} \tag{4}$$

$$F_{diss} = 0 \qquad \text{if} \quad \Omega \geq 1 \text{ at} \quad z = z_{\mathrm{max}} \tag{5}$$

$$F_{diss} = k_{\mathrm{diss}}(\Omega) \cdot F_{\mathrm{PIC}}(z_{\mathrm{max}}) \qquad \text{if} \quad \Omega < 1 \text{ at} \quad z = z_{\mathrm{max}} \tag{6}$$

Glossary

z	Water depth	z_{eup}	Bottom of euphotic zone
z_{max}	Bottom of the ocean	z_{lys}	Depth of lysocline
L_{PIC}	PIC degradation length scale	k_{PIC}	PIC dissolution rate const.
Ω	Saturation state	n	"Order" of the reaction
w	PIC sinking rate	F_{diss}	Dissolution flux at z_{max}
$k_{\mathrm{diss}}(\Omega)$	Carbonate dissolution related to saturation state		

Note: Models considering calcite and aragonite have seperate profiles, the sum of which is equal to the total PIC flux at each depth.

Figure 11: Overview of model approaches that are applied in paleoclimate models to calculate the depth profiles of PIC fluxes.

evoked as an explanation for the shallow dissolution (e.g., **????**), but no clear conclusions could be established. Alternative explanations involve more soluble forms of carbonates, such as aragonite or high-magnesium calcites (e.g., **??**). In summary, the dissolution of carbonates in the ocean is much more dynamic than our present understanding is able to explain.

3.2.3.2 Numerical approaches

This complexity is generally not reflected in the existing paleoclimate models. In fact, the applied approaches reflect much of the uncertainty that exists about the main drivers of calcium carbonate

dissolution in the global ocean. In general, two very different approaches for the simulation of PIC depth profiles are applied in paleoclimate models (Fig. 11). The majority of paleo-models simply assume an exponential decrease of the PIC flux below the euphotic layer. The applied degradation length scales are typically chosen to be broadly consistent with the PIC flux ratio inferred from observations by **?**, as well as **?** and fall within the range between 1000 m and 3000 m. The GENIE model assumes that a fixed fraction of the PIC export production reaches the deep ocean, while only the remaining fraction is subject to an exponential decrease with water depth. The magnitude of the respective fractions as well as the length scale are chosen consistent with the general conclusions of **?**, and more specifically, with the sediment trap observations of **?**. In HAMOCC for instance (**?**) the downward flux of $\mathrm{CaCO_3}$ is attenuated with a length scale of 2000m. However, for some applications (e.g. **?**), 30% of the carbonate export production was assumed to reach the sea-floor unchanged. In general, although able to represent calcium carbonate dissolution above the lysocline, the exponential model strongly simplifies calcium carbonate dynamics in the ocean. It is completely decoupled from the saturation state and organic carbon degradation dynamics, the most important drivers of calcium carbonate dissolution. Therefore, the exponential model cannot account for a dynamic response of the PIC flux profile to changing environmental conditions and its applicability to past extreme events is thus questionable. An alternative approach to the exponential model is based on the calcium carbonate reaction kinetics and is commonly used in diagenetic modelling. The overall process of calcium carbonate dissolution is a complex multi-step process. Although, the general rate law, R_{diss}, can be derived from thermodynamic and kinetic considerations (e.g. **?**), the most frequently employed rate law is empirically derived (**??**):

$$R_{\mathrm{diss}} = \left(\frac{A}{V}k\right) \cdot (1-\Omega)^n = k_{\mathrm{PIC}} \cdot (1-\Omega)^n \qquad \text{if } \Omega < 1 \tag{5}$$

where A is the total surface area of the solid, V is the volume of solution, $k_{(\mathrm{PIC})}$ is the rate constant and n is the apparent order of reaction. A synthesis of dissolution kinetics has shown that the apparent order of reaction varies between 1 and 4.5 (**???**). Some paleoclimate models (such as LOVECLIM and GEOCLIM *reloaded*) use a simpler version of the thermodynamic model. Instead of resolving the depth distribution of dissolution rate, they assume that calcium carbonate does not dissolve in the water column but solely at the bottom of the ocean (i.e. mimicking surface sediment dissolution.). The thermodynamic approach accounts for the direct link between the organic and inorganic carbon cycle. In addition, it allows a dynamic response of the simulated PIC flux to changes

in ocean chemistry and saturation state. Furthermore, its theoretical framework is based on a mechanistic understanding of the underlying thermodynamic and kinetic drivers. Yet, it does not account for the abundantly observed shallow carbonate dissolution and might thus underestimate the extent of calcium carbonate dissolution in the water column.

3.3 Benthic zone

At the seafloor, biogeochemical diagenetic processes are influenced by biogeochemical cycling in the overlying bottom water and the upper ocean. Dissolved species diffuse from the bottom water into the sediments and particulate material (such as organic matter, calcium carbonate or opal) rain down on the sediments and fuel biogeochemical reactions. Diagenesis transforms a substantial part of the deposited material (e.g. via remineralisation and/or dissolution) and the resulting products (e.g., DIC, nutrients) may return to the water column. As such, diagenetic processes are key components in the global carbon cycle as they trigger a delayed response to changes in ocean and atmosphere geochemistry and control the removal of carbon from the ocean reservoir (e.g. **??????**).

In marine sediments, carbon is buried as organic carbon or carbonate minerals (Fig. 12). Ultimately, only a small fraction of the organic carbon (generally 10–20% of the deposited organic carbon or less than $\sim$0.5% of the gross primary production) escapes remineralisation and is eventually buried in the sediment (e.g. **???**). However, organic carbon burial rates have been shown to vary significantly across different environments (e.g., **?**) and through geological history (e.g., **?**). The relative fraction of the deposited organic carbon that is ultimately buried in marine sediments can range from 0 to 100% (e.g., **?**). A plethora of different mechanisms has been proposed to explain the observed patterns of organic carbon burial in marine sediments but their relative importance remains elusive (**????**).

It has been shown that on a global scale, only 10–15% of carbonate produced escapes dissolution and is buried in accumulating sediments (**???**). Carbonate burial strongly depends on the saturation state of bottom- and porewaters. Because oceanic waters become increasingly less saturated at greater depth, deep-sea sediments are typically completely devoid of carbonate minerals. Furthermore, carbonate preservation is strongly influenced by the breakdown of organic matter and the release of metabolic CO_2 (**????**). Fig. 13 illustrates potential differences in carbonate dissolution fluxes as a function of bottom-water saturation (Ω) for two different scenarios. The first considers only bottom-water undersaturation, whereas the second takes bottom-water undersaturation and the

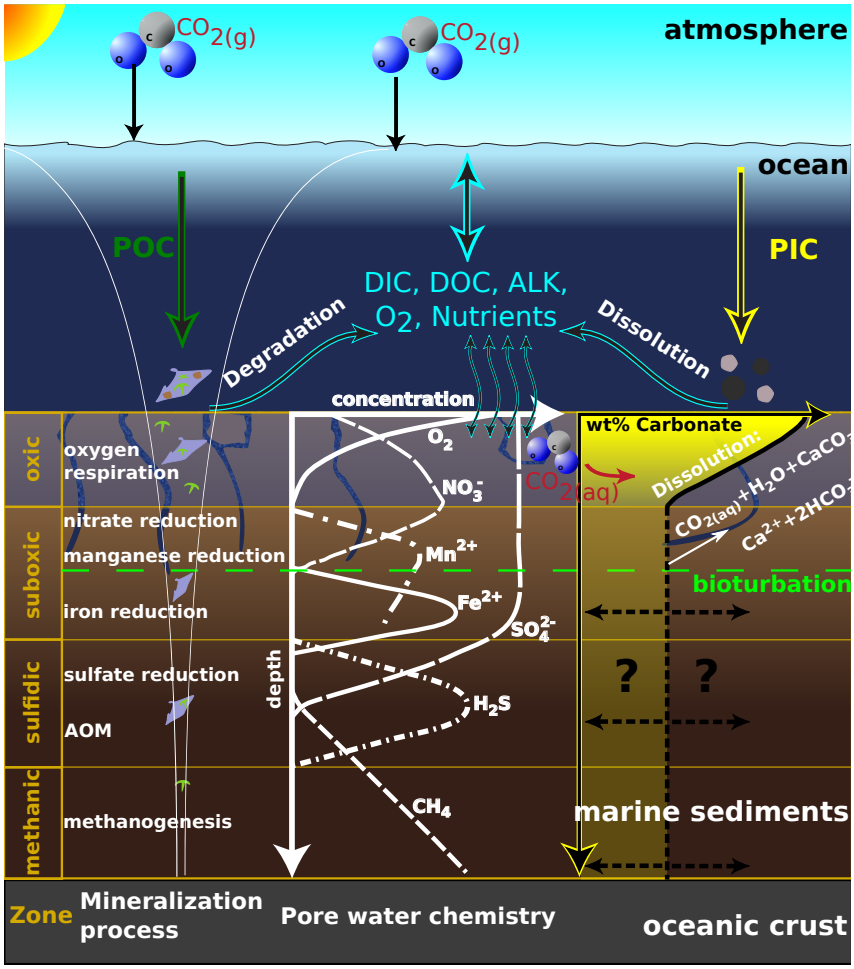

Figure 12: Schematic representation of the main early diagenetic processes and redox zonation in marine sediments. Typically sediments consist of several biogeochemical zones (left, as proposed by **?**). Oxygen, and other species, diffuse from the water column into the upper sediment layer (blue arrows, the oxic zone). Deeper layers are suboxic or anoxic (sulfidic, methanic), and are characterised by different reactions in which for instance nitrate, manganese(IV), iron(III) or sulfate ions are reduced (and re-oxidised). Exact depths, however, vary strongly and increase from the shelf to the deep sea. The depth sequence of the dominant remineralisation reaction of organic matter (in white, AOM: Anaerobic Oxidation of Methane) is reflected in the vertical pore water profiles of its reactants and products (white, concentration scales are arbitrary). Carbonate reaching the deep-sea sediments may dissolve during early diagenesis if the bottom water is undersaturated or if porewater metabolic processes (primarily aerobic degradation) cause further undersaturation in the sedimentary porewater (right).

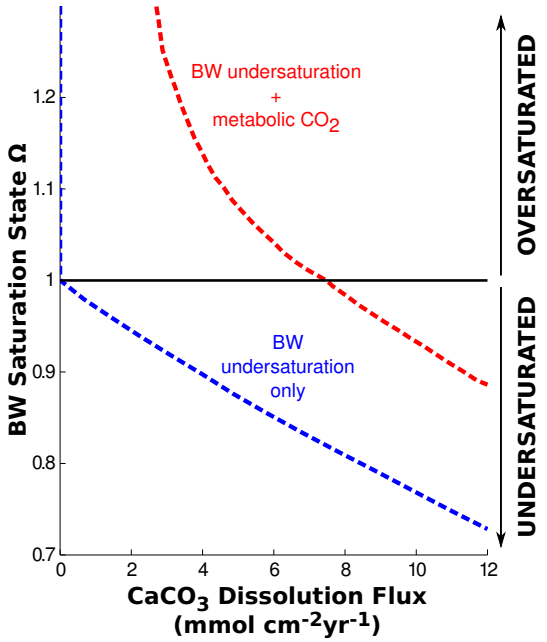

Figure 13: Calcite dissolution fluxes as a function of the degree of bottom water saturation, Ω. The blue dashed line represents the dissolution that would occur due to bottom-water undersaturation only, in the absence of any metabolic CO_2 (in analogy to the simplified thermodynamic model, Fig. 11). The red dashed line is the total carbonate dissolution (due to bottom-water undersaturation + organic carbon degradation) considering two organic carbon components and an average ocean-basin respiration rate. The two organic carbon component model represents a slower and faster decaying organic carbon pool in the sediments. Note that the scenario including the release of metabolic CO_2 drives more carbonate dissolution for all saturation states. Modified from **?**.

release of metabolic CO_2 into account. The burial fluxes and efficiencies of carbonates and organic carbon are thus strongly influenced by early diagenetic processes, as well as their feedbacks on ocean biogeochemistry (**???**).

In marine sediments, geochemical processes are tightly coupled and geochemical species may undergo several recycling and transformation loops (e.g., authigenic mineral precipitation/dissolution) before they are either buried or diffuse back to the water column. This complex process interplay complicates the interpretation of the sedimentary record, one of the major climate archives on Earth. Coupled paleoclimate models, which include a mechanistic description of all the feedback loops controlling the carbon dynamics, could provide powerful tools to unravel this process interplay, to

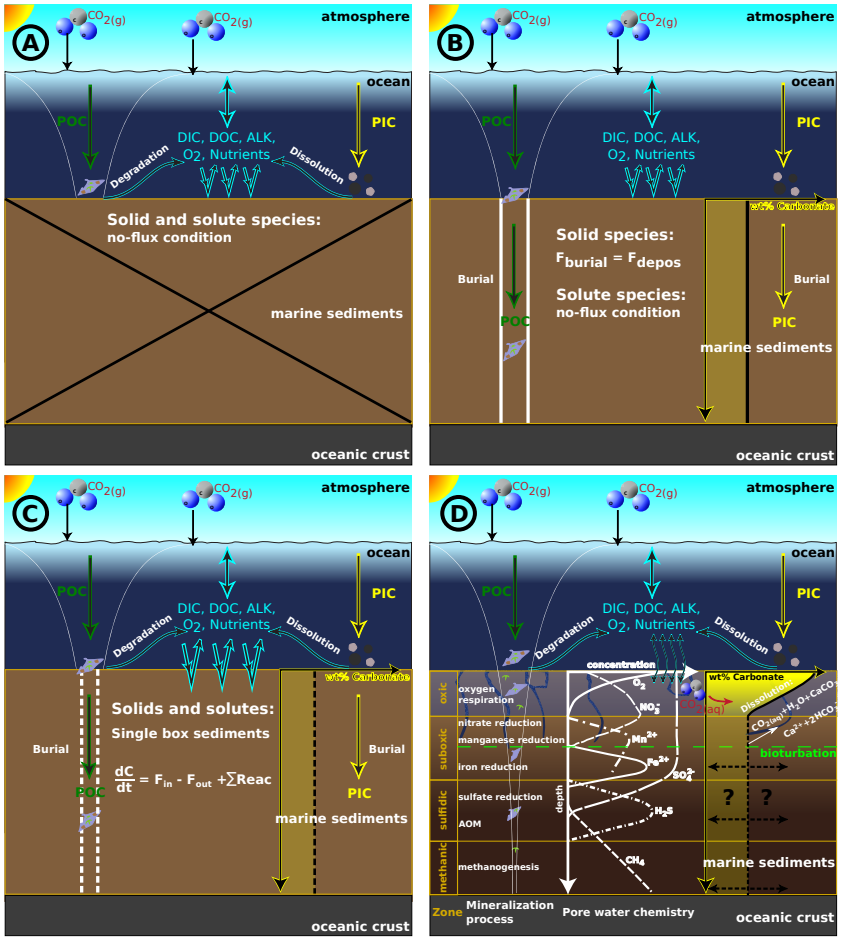

Figure 14: Schematic representation of the four different sediment approaches in paleoclimate models. Adapted from **?**. **A**: Reflective Boundary; **B**: Conservative/semi-reflective Boundary; **C**: Vertically-integrated, dynamic model; **D**: Vertically resolved, diagenetic model (same as Fig. 12).

enable a direct comparison between model results and observations and to test alternative hypotheses concerning the causes and effects of extreme perturbations of the global carbon cycle and climate.

However, although state-of-the-art early diagenetic models are sophisticated and comprehensive enough to accurately reproduce observations and predict exchange fluxes (see e.g. **??**), most paleoclimate models do not resolve the complexity of diagenetic processes. The primary constraint here is the high computation cost of simulating all of the essential redox and equilibrium reactions within marine sediments that control carbon burial and benthic recycling fluxes: a barrier that is exacerbated if a variety of benthic environments are to be spatially resolved. Instead, most models either neglect or only roughly approximate biogeochemical processes in the sediment and the benthic-pelagic cou-

pling. In the following, we describe model approaches for shallow-water coral reefs and, similar to results of an earlier review of the coupling between benthic and pelagic biogeochemical models (**?**), four representations for deep-sea sediments characterised by different levels of complexity (Fig. 14 and Fig. 15).

3.3.1 Shallow-water carbonate sediments

Not all burial of carbonates takes place in the deep-sea; it is currently estimated that approximately an equal amount accumulates in shallow-water (neritic) environments (**??**). Neritic carbonates are primarily the product of seafloor dwelling calcifying organisms such as corals, echinoids, mollusks, benthic foraminifera, bivalves, sea urchins, or coralline algae, whose long-term accumulation can result in the formation of large carbonate banks or reefs (e.g. **?**). As today the surface ocean is largely oversaturated with respect to aragonite (Ω_{Ar}), most of the global shallow-water carbonate production (about 0.65–0.83 Pg $\mathrm{CaCO_3}$ yr^{-1}, **?**, i.e., 0.078–0.100 Pg C yr^{-1}) is retained and accumulates in coral-reef sediments. Additionally, particulate organic carbon flux and sedimentation rates are elevated in neritic environments therefore often leading to suboxic and anoxic conditions in the sediments. The current knowledge is that the rate of calcification is controlled by a combination of ambient factors such as aragonite saturation state of the seawater, temperature and light availability (e.g. **???**). However, more research is needed in order to improve the understanding of the interplay of physico-chemical and biological factors controlling the formation and composition of shallow carbonates (**?**). In some paleoclimate models, such as GENIE (**?**), MBM (**??**) and GEOCLIM (**?**), shallow-water carbonate formation depends on the saturation state of the epicontinental ocean with respect to $\mathrm{CaCO_3}$, as well as on the total shelf area available for the formation of carbonate platforms (**?**) and possibly the rate of sea-level change (**??**). The majority of paleoclimate models, however, ignore carbonate deposition in shallow-water environments because of resolution issues and the high computational requirements to model the involved suboxic and anoxic redox-reactions.

3.3.2 Deep-sea Sediments

Paleoclimate models use a wide variety of approaches to represent ocean-sediment exchange fluxes. The most simple ones do not include any explicit sediment scheme, but simply assume that particulate fluxes reaching the bottom of the ocean degrade there, and the remineralisation or dissolution products return to the deepest model grid cells or boxes of the ocean. Remineralisation and/or disso-

Conservative/semi-reflective boundary

e.g. in LOVECLIM (Goosse et al., 2010)

$$F_{\mathrm{S,bur}} = F_{\mathrm{S,dep}} \qquad (\text{ or } \alpha \cdot F_{\mathrm{S,dep}}) \tag{1}$$

$$F_{\mathrm{D,rf}} = 0 \qquad (\text{ or } R \cdot (1-\alpha) \cdot F_{\mathrm{S,dep}}) \tag{2}$$

$$\alpha \in (0,1], \text{ (with } \alpha = 1 \text{ for the conservative boundary)}$$

$$C_{\mathrm{D,sed}} = 0 \tag{3}$$

Reflective boundary

e.g., in Bern2.5D (Marchal et al., 1998b) and GENIE (Ridgwell et al., 2007):

$$F_{S,\mathrm{bur}} = 0 \tag{4}$$

$$F_{D,\mathrm{rf}} = g\left(F_{S,\mathrm{dep}}\right) \qquad (\text{ or } R \cdot F_{S,\mathrm{dep}}) \tag{5}$$

$$C_{D,\mathrm{sed}} = 0 \tag{6}$$

Vertically-integrated, dynamic model

e.g., in Bern3D (Tschumi et al., 2011), LOSCAR (Zeebe, 2012) or MBM1996 (Munhoven and François, 1996):

$$F_{S,\mathrm{bur}} = F_{S,\mathrm{dep}} - \sum_j Reac_j \tag{7}$$

$$F_{D,\mathrm{rf}} = \sum_j \beta_j Reac_j \tag{8}$$

$$\frac{dC_{D,\mathrm{sed}}(t)}{dt} = F_{\mathrm{D,in}} - F_{D,\mathrm{out}} + \sum_j (1-\beta_j) Reac_j \tag{9}$$

Vertically resolved, diagenetic model

General steady-state diagenetic equation for solid and dissolved species C_i after Berner (1980).
See e.g. GEOCLIM *reloaded* (Arndt et al., 2011):

$$\begin{aligned} \frac{\partial \xi C_i(t,z)}{\partial t} = 0 &= -\frac{\partial}{\partial z} F + \xi \sum_j Reac_j \\ &= -\frac{\partial}{\partial z}\left(-\xi D_i \frac{\partial C_i}{\partial z} + \xi w C_i\right) + \xi \sum_j Reac_j \end{aligned} \tag{10}$$

Glossary

S	Solid species	D	Dissolved species
$F_{S,\mathrm{bur}}$	Sediment burial flux of solids	$F_{i,\mathrm{dep}}$	Bottom water deposition flux of i
$F_{D,\mathrm{rf}}$	Dissolved return flux	$C_{D,\mathrm{sed}}$	Sediment concentration of D
	due to OM remineralisation	$F_{D,\mathrm{in/out}}$	General dissolved in/out-flow
α	Fraction of solids preserved	R	Stoichiometric ratio
$g()$	Steady state return flux	$\beta_j \in [0,1]$	Dissolved fraction returned to ocean
z	Sediment depth	z_{max}	Maximum sediment depth
$\sum_j Reac_j$	Sum of relevant production	ξ	Equals porosity ϕ for solutes and
	/consumption processes		$(1-\phi)$ for solids
F	Transport fluxes	D_i	Diffusion coefficient
w	advection rate		

Figure 15: Overview of applied model approaches to calculate burial of solid species (i.e. PIC and POC), return/recycling fluxes of dissolved species resulting from organic matter (OM) remineralisation and sediment concentrations of dissolved species.

lution may be either complete or partial. In the latter case, the non-degraded fraction is returned to the surface ocean, to mimic riverine input, thus avoiding the model drift because of global inventory changes. POC remineralisation rates may be dependent on oxygen concentrations in the grid cells just above the seafloor and PIC dissolution rates on the saturation state with respect to the saturation state of bottom waters. Some models (e.g. BICYCLE) use a restoration scheme, either based upon a prescribed history of the sedimentary lysocline, which is used as a proxy for the calcite saturation horizon (**?**) or a reference deep-sea CO_3^{2-} concentration (**?**). Even models with explicit representations of the surface sediments exhibit a large variety of configurations: Along the vertical in the sediment column, complexity ranges from single-box surface mixed-layers (e.g., **?**) to well resolved sediment columns (e.g., 21 grid-points for the surface mixed-layer in MEDUSA, **?**). Underneath the mixed-layer, some models additionally track the history of preservation in synthetic sediment cores (e.g., **?**). The composition of the model sediments is also highly variable, encompassing the range from a minimalistic calcite-clay mixture (**??**) with an implicit, steady-state porewater $[CO_3^{2-}]$ profile, to a composition that essentially reflects the ocean model tracer (e.g. DIC, O_2, PO_4) in porewaters and material fluxes (e.g. PIC, POC, $CaCO_3$, opal and clay) in the solid fraction (Bern 3D, **?**). Except for MEDUSA in MBM (**?**), no sediment model appears to explicitly consider aragonite as a sediment constituent. In other models, the entire aragonite flux is dissolved close to the sediment-water interface if bottom waters are undersaturated with respect to aragonite, while the flux is entirely preserved in oversaturated bottom waters, possibly "converted" to calcite (e.g. in MBM, **?**). The various adopted approaches may be divided into four major classes, which we review in the following.

3.3.2.1 Reflective Boundary

The Bern 2.5D model includes the sediment-water interface in form of a reflective boundary (**?**) and also the GENIE model provides this as an option (**?**) (Fig. 14A). The deposition flux of PIC and POC that would settle onto the sediments is completely consumed in the deepest ocean cell, instantaneously releasing dissolved carbon and nutrients. This approach is, due to its computational efficiency, often used in global biogeochemical models (e.g. **???**). Usually the partitioning of the return flux (representing benthic transformations) is parametrised or calculated based on steady-state diagenetic modelling (**??**). As the reflective boundary approach does not model any benthic PIC and POC burial fluxes it overestimates benthic recycling fluxes and completely neglects the

strong coupling between POC and PIC fluxes through the effect of organic matter degradation on carbonate dissolution (Fig. 13). In addition, it does not account for the temporal storage of material in the sediment and the time delay between deposition and recycling flux. Therefore, this highly simplified approach cannot resolve the complex benthic-pelagic coupling.

3.3.2.2 Conservative/semi-reflective Boundary

The conservative boundary approach (Fig. 14B) refers to biogeochemical models that impose burial fluxes and sediment-water exchange fluxes. In general, the burial flux of PIC and POC is set equal (or proportional) to their deposition flux. In addition, a no-flux boundary condition is applied for solute species, neglecting any exchange through the sediment-water interface. For instance LOVE-CLIM incorporates such a sediment model where a constant part of POC and PIC is preserved (**?**). The conservative nature of this approach does not violate mass conservation and accounts for the retention capacity of sediments. Nevertheless, it neglects (or oversimplifies) the degradation of POC and the dissolution of PIC in marine sediments and thus overestimates (or crudely approximates) the burial fluxes. In addition, such a simplified approach does not represent the time-delayed recycling of nutrients and dissolved carbon and the impact of these fluxes on the biogeochemical functioning of the ocean-atmosphere system. Another important caveat of this approach is that it cannot account for a change in speciation. Generally, the composition of the benthic return fluxes is fundamentally different from the composition of the deposition flux (e.g. **?**). In marine sediments, the coupled redox-reactions, mineral precipitation/dissolution or equilibrium reactions control the speciation. The exact composition of the total dissolved carbon flux, for instance, strongly depends on the vertical distribution of biogeochemical reaction rates and their combined influence on the ambient pH. The conservative boundary approach does not capture this biogeochemical complexity and thus does not appropriately represent the sedimentary response.

In order to illustrate how different sediment boundary conditions affect biogeochemistry in the ocean we compare a GENIE set-up using the reflective boundary with the conservative boundary for two climate scenarios (see Box 2 for more information). The impact of including organic carbon burial on global mean water-column O_2 and PO_4 concentration during the Eocene is shown in Fig. 16 (A+B). Global deep water O_2 concentration increases as POC reaching the seafloor is buried and not remineralised. In contrast, nutrient concentration in the deep ocean is decreasing as less PO_4 is released to the ocean. But not just the global O_2 concentration changes, also the spatial difference of

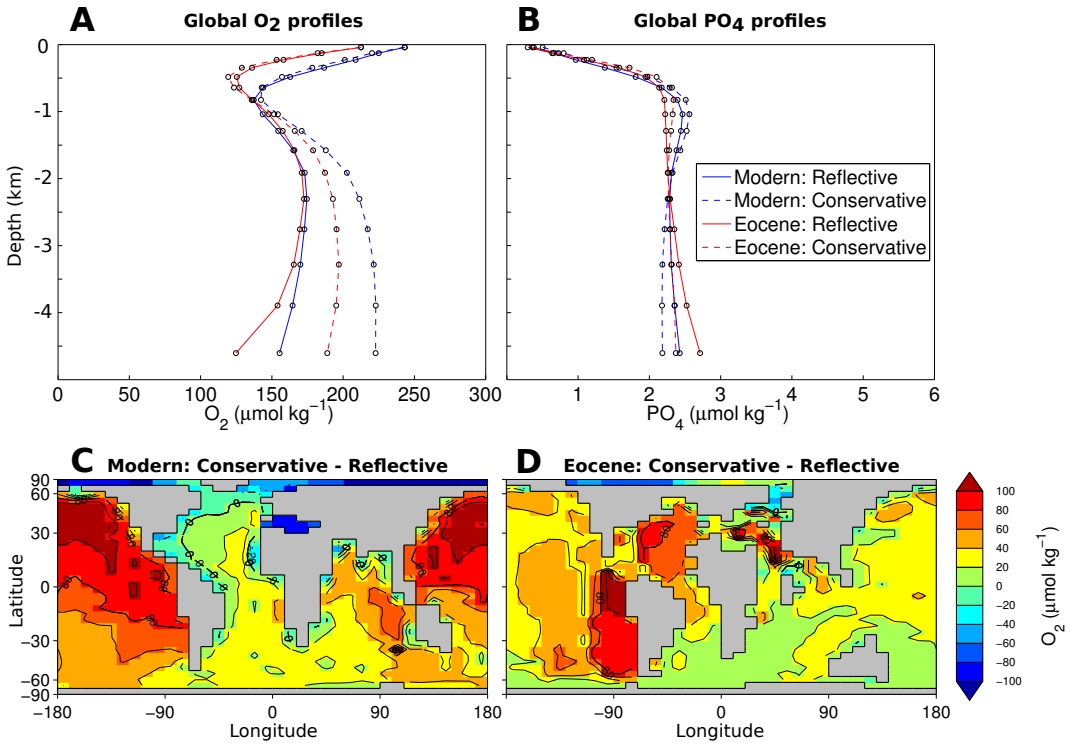

Figure 16: Model comparison of marine biogeochemistry with GENIE configurations using the Conservative and Reflective sediment approach for the modern and Eocene world. Modelled global oxygen (A) and phosphate (B) profiles. (C+D): Anomaly plots (Conservative minus Reflective) of bottom water oxygen concentration for modern (C) and Eocene (D) world.

bottom water oxygenation for the two sediment schemes varies significantly for the modern and the Eocene (Fig. 16C+D). Ocean redox differences are even more pronounced when applying the two sediment representations for the Late Cretaceous. Fig. 17 (A) highlights the problem of the reflective lower boundary by showing an unrealistically high concentration of H_2S at the seafloor. This result is an artifact of the lower boundary condition as all POC gets instantaneously remineralised at the seafloor. On the other hand, the conservative boundary (Fig. 17B) shows very little H_2S in the deeper ocean as it neglects completely the degradation of POC at the seafloor. However, the employed lower boundary condition does not only have implications on redox conditions at the bottom of the ocean but can also be seen in the photic zone (Fig. 17C).

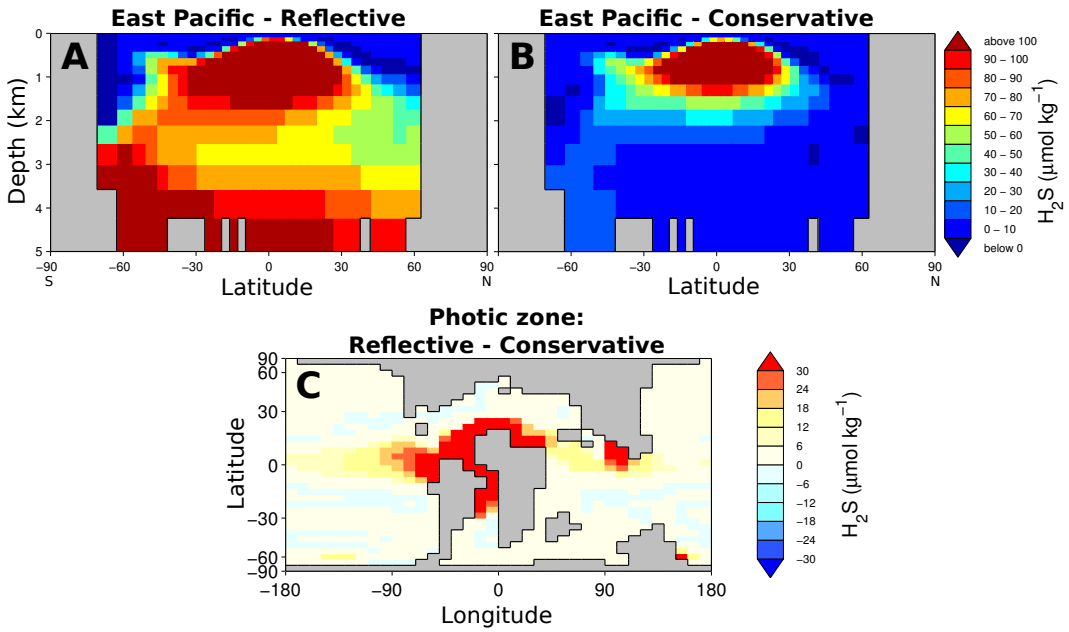

Figure 17: Model comparison of H_2S concentration during OAE2 with GENIE configurations using the Conservative and Reflective sediment approach. (A+B): Vertical profile of H_2S in the East Pacific Ocean ($-90°$ longitude). (C): Anomaly plots (Reflective minus Conservative) of photic zone euxina (i.e. H_2S concentration for 80-200m depth).

3.3.2.3 Vertically-integrated dynamic model

In the vertically-integrated approach, the sediment is represented as a single box (Fig. 14C). The average concentration of the represented species in this box is calculated as the balance between the deposition and burial flux, as well as the sum of consumption processes. The diffusive flux of dissolved species through the sediment-water interface in turn equals the sum of consumption/production processes that are usually tightly linked to the transformation of particulate material (e.g. **?**). The model thus neglects temporary storage of dissolved species and fluxes in porewaters. However, this approach is clearly superior to the two simpler approaches. It has the merit of simplicity and is computationally efficient. In addition, it also reproduces some of the complexity associated with the short- and long-term evolution of benthic recycling fluxes. Such an approach also allows differentiating between various fractions of organic matter (if POC is represented) and therefore is able to resolve some of the biogeochemical complexity associated with the decrease of organic matter reactivity with sediment depth. Most paleo-EMICs incorporate a vertically-integrated sediment model for PIC

only, sometimes considering oxic-only sediment respiration of organic carbon (compare Tab. 2). Bern 3D being a notable exception, as it includes a vertically-integrated dynamic model also considering oxic degradation and denitrification of organic carbon (**?**),

3.3.2.4 Vertically resolved diagenetic model

So-called diagenetic models provide the most robust description of the benthic-pelagic coupling (Fig. 14D). Those models solve the one-dimensional, fully coupled reaction-transport equation for solid and dissolved species (e.g. **??**). This approach thus accounts for all important transport processes, such as burial, compaction, bioturbation, molecular diffusion and bioirrigation. In addition it resolves the fully coupled biogeochemical dynamics of the carbon, oxygen and nutrient cycles and the resulting characteristic redox-zonation of marine sediments (also compare Fig. 12). However, controversy still revolves around the formulations of organic matter degradation (e.g. **?**) and calcite dissolution (e.g. **?**). In addition, the parametrisation of diagenetic models requires a good understanding of diagenetic dynamics and careful consideration of the environmental conditions. For instance, rate constants that are typically used in state-of-the art diagenetic models may predict the benthic response in the modern-day, well ventilated ocean, but might not be applicable under extreme environmental conditions such as OAEs or the PETM. The major drawback of those models is the computational cost associated with the computation of vertically-resolved reaction-transport equations for a number of interacting species. Therefore, paleoclimate models that include a diagenetic model generally reveal a very low spatial resolution of the benthic environment (e.g. GEOCLIM *reloaded* only resolves three sediment columns; **?**) or use other methods to reduce computational demands: DCESS for instance uses a semi-analytical, iterative approach considering $\mathrm{CaCO_3}$ dissolution and (oxic and anoxic) organic matter remineralisation (**?**). One exception here is the early diagenesis model MEDUSA which is coupled to the multi-box model MBM (**?**). MEDUSA operates in a fully transient way at 100 m depth intervals over the whole model sea-floor, in five regions, totalling 304 columns.

3.3.3 Conclusion

Marine sediments represent the largest reservoir of carbon among the exogenic reservoirs (**?**). The assessment of the response of the ocean to variabilities in atmospheric $\mathrm{CO_2}$ concentrations requires a robust quantification of the benthic-pelagic coupling and the sedimentary carbon sink (**????**). How-

ever, it appears that convenience rather than a careful mechanistic representation and the ability of the approach to provide an answer to the problem guides the choice of the lower boundary condition for the ocean model. Paleoclimate modelling has developed to a stage where increasingly complex and multi-dimensional ocean, atmosphere and continental vegetation models are coupled (e.g. **??**). Yet, compared to these developments, considerably less effort has been devoted to the coupling between ocean and sediment models. However, sophisticated, comprehensive and carefully calibrated and tested diagenetic models (e.g. **????**), as well as computationally efficient pseudo dynamic approaches (e.g. **??**) are now available and could be incorporated into paleoclimate models in numerically efficient ways, such as for instance look-up tables (see e.g. **?**) or neural networks (see Section 4.3). Ultimately, our ability to understand past climate change critically depends on a better quantification of the sedimentary carbon sink and its response to extreme environmental conditions (**????**).

4 Conclusions and future directions

The biological pump in the ocean involves biology, chemistry and physics and is a dynamic system that evolves over time in association with a changing climate. The mechanistic understanding of the processes involved has improved significantly, however, a quantitative assessment of the importance of different mechanisms is still lacking. Rather than solely using existing, static numerical representations for the biological pump and trying to reproduce certain paleo-observations as perfectly as possible (which is in essence often just a fitting exercise), paleoclimate models should also be used to explore new methodologies and biogeochemical mechanisms to test our comprehension of the dynamical behaviour of the biological carbon pump. Reviewer 2: ... statement not as trivial as it seems at first glance and need to be discussed.. Despite the increased number of paleoclimate models incorporating marine carbon cycle dynamics and the improved understanding of the biological pump, mathematical formulations of these processes have not considerably evolved at the same time. The organic and inorganic carbon cycling in the ocean and the benthic-pelagic coupling are still represented by highly simplified approaches and are therefore of limited transferability across time and space. Progress in understanding past climate variations will crucially depend on the combined use of different representations (e.g. conceptual and mechanistic) of the surficial carbon cycle and the quantification of related model uncertainties. The following paragraphs highlight the role of using models of different complexities (4.1), give suggestions how these models can be applied to explore

and quantify different model uncertainties (4.2), and identify two major challenges to help direct future research for the paleoclimate (modelling) community (4.3).

4.1 The importance of different models

Fundamentally, mathematical models are always approximations of the complex, real Earth system and all assumptions are erroneous on some level (**?**). For instance, assuming a reflective sediment-water interface is appropriate when investigating carbon cycle processes on time scales shorter than 1000 years but is misleading when studying longer time scales. A box model approach is helpful when trying to isolate the dominant process in an observed global or large-scale output but not very helpful when one is interested in a more detailed (spatial) analysis of a problem (e.g. modelling marine ecology which is dependent on local transport and mixing processes and the spatial resolution of the ocean).

Both model types (i.e. structurally simple or conceptual models and more coupled or mechanistic models) have their advantages and disadvantages (compare e.g. **?**). The structural simplicity of box models considerably reduces the models dependency on initial and boundary conditions and the model is easier to constrain as it includes fewer parameters and variables. Due to their lower computational demand box models can be used for large-ensemble experiments needed to address important questions regarding uncertainty quantification (see Section 4.2). Also, the output is less complex, easier to interpret and therefore may provide a clearer understanding of the dominant process. However, there is a higher possibility of misinterpreting the *real* process if it is actually the product of several interacting effects not represented in the model. Furthermore, the simplicity of the model (in terms of resolution and represented processes) usually restricts the development of emergent behaviours. More coupled or mechanistic models provide a more accurate view of the interrelated real system's dynamics and, therefore, have a stronger predictive ability. However, simply including more and more complexity (in the sense of additional mechanisms) does not guarantee an improvement of the predictive ability of the model. It may even reduce it, if the new representation is based on over fitting imprecisely known free parameters to limited observations (**?**). Thus, a crucial step is to show that the representation of the new mechanism has an acceptable level of accuracy over a range of conditions.

Improving mechanistic parametrisation of key processes is one of the main challenges that hinder better understanding in Earth sciences. That, however, does not undermine the value of non-

mechanistic models (e.g. conceptual, mathematical, statistical or numerical) that have no predictive ability. Starting an investigation with a simple model and gradually increasing its complexity can reveal emerging model and system behaviours which might have been overlooked when employing the most complex model alone (compare **?**, for an example). Also model structure within a modelling approach is not unique, as has been demonstrated in this review. These different models and their results can provide valuable insights into the significance of model structure (i.e. structural uncertainty; see Section 4.2). We recommend, in order to gain better scientific understanding, to use a range of different models and/or mathematical representations when examining a problem and to know the limits and uncertainties for the models being used as accurate as possible.

4.2 Quantifying uncertainty

Beside being ideal tools for testing our understanding of the biological carbon pump and for exploring the long-term carbon cycle evolution, paleoclimate models should further be used to investigate uncertainties related to modelling climate and marine carbon cycle feedbacks and to identify which processes have the greatest influence upon model predictions. Currently uncertainty estimates for the climate-carbon cycle response are primarily done using different future emission scenarios (e.g. **???**) or, where possible, by comparing model results with observational uncertainty estimates (e.g. **??**). In the case of model intercomparison projects mainly simplified characteristics such as the ensemble standard deviation or range are used (e.g. **???**) or EMIC results are compared with results obtained from GCMs (e.g. **???**). In the following, we summarise different types of uncertainties the modelling community has to deal with and give suggestions for how different numerical models can be used to explore them.

Uncertainty in (Earth system) modelling can generally be considered as a lack of knowledge or information concerning the processes involved and comes from a variety of sources (**??**). First, input uncertainty, that is the uncertainty caused by errors in the boundary conditions, such as continental configuration, bathymetry, oceanic nutrient concentration or atmospheric CO_2 forcing. Second, parameter uncertainty, introduced through uncertain estimates of model parameters or because the optimal parameter set is ambiguous. And third, model structural uncertainty, resulting from simplifications, discretizations, inadequacies or ambiguities in the numerical representation of the real process. The different sources of uncertainty generally vary with model complexity (Fig. 18). Ideally, as more processes are described in the model (i.e. an increase in model complexity) the structural un-

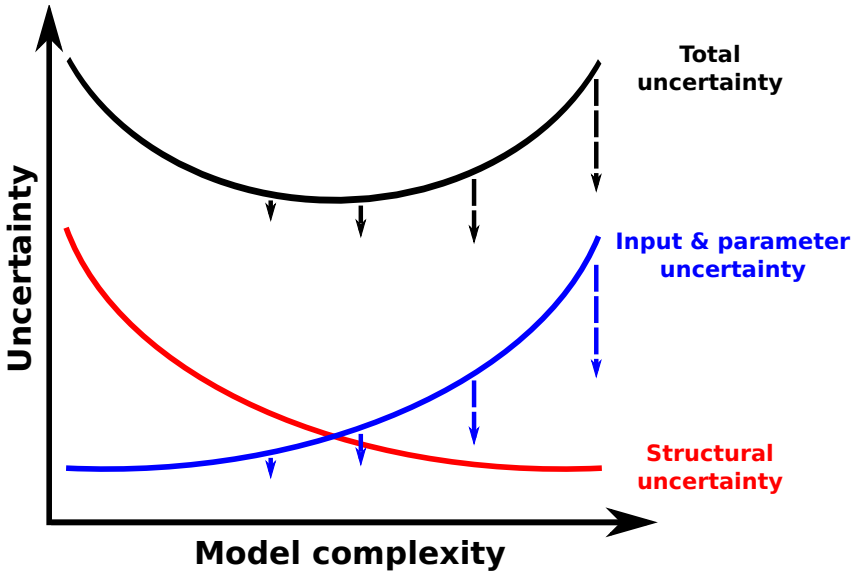

Figure 18: Idealised dependency of various sources of uncertainty on model complexity (i.e. components, resolution and represented processes). Blue arrows depict an improvement of input or parameter uncertainty using SA and empirical methods (see text) which results in a decrease in total model uncertainty (black arrows). Adapted from **?**.

certainty of the model decreases. However, at the same time more parameters and inputs are needed to describe and/or constrain these processes, therefore increasing input and parameter uncertainty. Due to this trade-off between different complexities there is theoretically an optimal model for every given real world problem characterised by minimal total uncertainty. Obviously, this is an idealised example and in reality it is not possible to decide which model is the optimal one, especially in the case of paleoclimate modelling where validation against observations is limited.

One strategy to explore and quantify model uncertainty that can always be applied is sensitivity analysis (SA). **?** deliver a comprehensive review of SA methods most widely used in other environmental modelling fields. They also provide practical guidelines for choosing the most appropriate SA method for a specific problem, depending on the purpose of the analysis and the computational complexity of the method. Sensitivity analysis in combination with empirical approaches can also be used to iteratively reduce the uncertainty for a given numerical model (compare e.g. **?**). For instance in the case of parameter uncertainty, SA can identify which parameters have the greatest influence upon model output and how constrained their values are. Mechanistic parameters with explicit relevance to biology or physics (such as degradation rate constants, activation energies and temperature

dependencies) may then be better constrained empirically using laboratory experiments or more observations, thus decreasing parameter uncertainty (compare Fig. 18). However, more conceptual parameters (e.g. Martin's b-value), that implicitly account for various processes, are more specific to individual model formulations and have to be determined by fitting each model to observations. The lack of correlation between these abstract parameters and real biogeochemical processes leads to an increase in parameter uncertainty (i.e. decrease in predictive ability) if the numerical model is applied under different environmental conditions. SA should be applied here to quantify this uncertainty.

Currently most studies treat only parameter uncertainty as source of uncertainty. However, research in hydrological modelling has shown that input or structural uncertainty can be even more important (**??**). Therefore, other questions concerning input and structural uncertainty should be explored more often using SA: How much does it matter if we change boundary conditions or forcings? What is the uncertainty in model results due to missing or oversimplified biogeochemistry? The computational efficiency of paleoclimate models (especially of box models) facilitates large simulation ensembles and systematic sensitivity studies thus allowing the estimation of these uncertainties using objective statistical methods. **?** and **?** for example present extensive sensitivity experiments to assess the skill of different global marine biogeochemical models for the modern ocean. Biogeochemistry in paleoclimate models will improve further in the future, representing more processes in greater detail. If in addition a higher confidence in their simulations is to be achieved these new processes need to be evaluated using objective methods. Therefore, besides exploring the parameter space, different representations of the biological pump should be tested against each other and evaluated with observations. Closer collaboration with statisticians to improve uncertainty analysis would be a step in the right direction and much can be learned from other disciplines such as engineering or hydrology where sensitivity analyses of numerical models are widely used (e.g., **??**).

4.3 Outstanding modelling issues

As shown in this study, a major problem of the presented models is the lack of theoretical frameworks that allow the parametrisation of particulate organic carbon flux under changing environmental conditions. Different generic algorithms for this parametrisation, based on current process understanding, are needed to resolve changes in the efficiency of the biological pump which is observed over time (e.g., **???**) and in space (e.g., **?**). Although the basic power-law or double-exponential decrease

in POC flux with depth has been abundantly demonstrated and is widely accepted, there is a strong need to link changes in downward particulate flux to the mechanistic understanding of the underlying processes. The results of different representations should be compared against each other as discussed above.

Another outstanding issue are the current oversimplified sediment representations in paleoclimate models, which are often not able to model the properties needed for a comparison to proxy-observations. One of the biggest barriers for a direct, dynamic coupling of sediment models is the high computational cost of simulating the whole suite of essential redox and equilibrium reactions within marine sediments that control carbon burial and benthic recycling fluxes. To overcome comparable problems, offline coupling approaches are often used. For instance, sophisticated atmospheric models such as FOAM are often run for a wide range of different atmospheric CO_2 concentrations. Based on these stand-alone simulations, look-up tables are created that link the modelled climatic conditions (e.g. precipitation, temperature) to atmospheric CO_2 (e.g., **?**). These look-up tables are numerically efficient representations of the full model that can subsequently be used in EMIC simulations to simulate the climatic response to changing atmospheric CO_2 concentrations. Artifical neural networks (which represent more sophisticated look-up tables or transfer functions that allow linking a number of input parameters to a number of output parameters) can be used to encapsulate a numerically cost intensive model in a similar way. A neural network encapsulation of sediment dynamics has to be trained using example bottom water conditions and related burial and benthic recycling fluxes calculated by a full diagenetic model. Instead of following static, human prescribed rules, neural networks have the ability to learn automatically the underlying relationship from the training set and are practically able to approximate any relationship between input and output properties (**??**). These approaches thus allow a full, dynamic coupling at a significantly reduced computational cost.

A Earth Sytem Model applications

Table 6: **Paleoclimate model applications (EMICs)** (ordered from higher to lower ocean resolution) with a relation to the biological pump. Study-time reflects the broad modelled time in the experiments (not the official timing of the event).

Model	Event	Study-Time	References
EMIC			
UVic	Last deglaciation	ca. 20 – 15 kyr BP	**?**
	Last deglaciation	23 kyr BP – present	**?**
	LGM	ca. 21 kyr BP	**??**
			?
	DO-event 8 & 12	ca. 37 & 45 kyr BP	**?**
	DO-event	universally	**??**
	Panama seaway closure	ca. 14 – 3 Ma	**?**
	Antarctic Glaciation	ca. 33.7 Ma	**?**
	PETM	ca. 55.8 Ma	**??**
			?
	End-Permian	ca. 252 Ma	**?**
LOVECLIM	Last deglaciation	ca. 21 – 10 kyr BP	**?**
	LGM	ca. 22.5 kyr BP	**???**
	Interglacials	universally	**?**
	Emian interglacial	ca. 129 – 118 kyr BP	**?**
Bern 3D	Holocene	ca. 8 kyr BP – present	**??**
	LGM and deglaciation	20.0 kyr BP – present	**??**
	Last glacial period	ca. 70 – 30 kyr BP	**?**
	Last glacial cycle	125 kry BP – present	**?**
	Emian interglacial	126 – 115 kyr BP	**?**
MESMO	Younger Dryas	ca. 12.9 – 11.7 kyr BP	**?**
	Heinrich 1	ca. 17.5 – 14.5 kyr BP	**?**
	LGM	ca. 22.5 kyr BP	**??**
	Glacial cycles	ca. 400 kry BP – present	**?**
GENIE	Holocene	8 – 0.5 kyr BP	**?**
	Younger Dryas	13.5 – 11.5 kyr BP	**?**
	Emian interglacial	126 – 115 kyr BP	**?**
	Eocene hyperthermal	49.2 Ma	**?**
		ca. 50 Ma	**?**
	Early Eocene	ca. 55 Ma	**??**
			?

A1

Table 7: **Table 6 (continued)**

Model	Event	Study-Time	References
GENIE	PETM	ca. 55.8 Ma	**??**
			??
			?
			?
	OAE2	93.5 Ma	**?**
	Cretaceous	101 Ma	**?**
	End-Permian	ca. 252 Ma	**??**
			??
	Last 400 Ma	400 Ma – present	**?**
CLIMBER-2	Holocene	ca. 8 kyr BP – present	**??**
	8.2 kyr BP event	8.2 kyr BP	**?**
	Last deglaciation	ca. 18 – 9 kyr BP	**?**
	LGM	ca. 21 kyr BP	**???**
			???
	Emian interglacial	ca. 125 kyr BP	**?**
		ca. 126 – 116 kyr BP	**??**
	Glacial cycles	126 kyr BP – present	**?**
	MIS 11 interglacial	420 – 380 kyr BP	**?**
GEOCLIM	Cretaceous	145.5 - 65.5 Ma	**?**
	Jurassic	199.6 – 145.5 Ma	**?**
	Triassic	251.0 – 199.6 Ma	**??**
	Late Neoproterozoic	580.0 Ma	**?**
	Neoproterozoic	1,000 – 542.0 Ma	**?**
MoBidiC	LGM	ca. 22.5 kyr BP	**?**
	Heinrich events	ca. 60 – 12 kyr BP	**?**
	& Last deglaciation		
Bern 2.5D	Younger Dryas	ca. 13.0 – 11.0 kyr BP	**???**
	Heinrich events	ca. 60 – 12 kyr BP	**?**
	& Last deglaciation		

Acknowledgements. DH is supported by a graduate teaching studentship by the University of Bristol. SA is supported by funding from the European Unions Horizon 2020 research and innovation programme under the Marie Skłodowska-Curie grant agreement No 643052. JDW and AR acknowledge funding from the EU grant ERC-2013-CoG-617313. GM is a Research Associate with the Belgian Fonds de la Recherche Scientifique-FNRS. Finally, we would like to thank Sarah Greene for helpful discussions.

2

Table 8: **Paleoclimate model applications (Box models)** (ordered from higher to lower ocean resolution) with a relation to the biological pump. Study-time reflects the broad modelled time in the experiments (not the official timing of the event).

Model	Event	Study-Time	References
Box			
DCESS	LGM	ca. 22.5 kyr BP	**?**
	PETM	ca. 55.8 Ma	**?**
SUE	since LGM	ca. 22.5 kyr BP – today	**?**
	Glacial cycles	400 kyr BP – present	**??**
	Snowball Earth	around 650 Ma	**?**
	Phanerozoic	600 Ma – present	**?**
CYCLOPS	LGM	ca. 22.5 kyr BP	**???**
			?
	Last deglaciation	ca. 30 kyr BP – present	**??**
	Glacial cycle	150 kyr BP – present	**??**
PANDORA	Glacial-Interglacial CO_2	universally	**???**
			?
LOSCAR	Mid-Miocene	16.8 – 13.8 Ma	**?**
	MECO	ca. 40 Ma	**?**
	Paleocene-Eocene	62 – 48 Ma	**?**
	Early Eocene	ca. 55 Ma	**?**
	PETM	ca. 55.8 Ma	**??**
			??
			??
			?
BICYCLE	Last deglaciation	21 – 10 kyr BP	**?**
	Glacial cycles	120 kyr BP – present	**?**
	Glacial cycles	740 kyr BP – present	**??**
	Mid Pleistocene Transition	2 Ma – present	**?**
MBM	Glacial cycle	ca. 150 kyr BP – present	**??**
			?

References